

# On the Mechanism Underlying the Spontaneous Emergence of Barotropic Zonal Jets

NIKOLAOS A. BAKAS AND PETROS J. IOANNOU

*Department of Physics, National and Kapodistrian University of Athens, Panepistimiopolis Zografos, Athens, Greece*

(Manuscript received 31 December 2011, in final form 17 December 2012)

## ABSTRACT

Zonal jets are commonly observed to spontaneously emerge in a  $\beta$ -plane channel from a background of turbulence that is sustained in a statistical steady state by homogeneous stochastic excitation and dissipation of vorticity. The mechanism for jet formation is examined in this work within the statistical wave–mean flow interaction framework of stochastic structural stability theory (SSST) that makes predictions for the emergence of zonal jets in  $\beta$ -plane turbulence. Using the coupled dynamical SSST system that governs the joint evolution of the second-order statistics and the mean flow, the structural stability of the spatially homogeneous statistical equilibrium with no mean zonal jets is studied. It is shown that close to the structural stability boundary, the eddy–mean flow dynamics can be split into two competing processes. The first, which is shearing of the eddies by the local shear described by Orr dynamics in a  $\beta$  plane, is shown in the limit of infinitesimal shear to lead to the formation of jets. The second, which is momentum flux divergence resulting from lateral wave propagation on the nonuniform local mean vorticity gradient, is shown to oppose jet formation. The upgradient momentum fluxes due to shearing of the eddies are shown to act exactly as negative viscosity for an anisotropic forcing and as negative hyperviscosity for isotropic forcing. The downgradient fluxes due to wave flux divergence are shown to act hyperdiffusively.

## 1. Introduction

Zonal jets are prominent features of planetary, turbulent flows with well-studied examples being the banded winds of the gaseous planets (Ingersoll 1990). These large-scale flows are maintained by the momentum fluxes of the turbulent eddy field with which they coexist (Kuo 1951; Starr 1968; Vasavada and Showman 2005) and emerge spontaneously out of a background of homogeneous turbulence both in rotating-tank experiments (Read et al. 2004) and in a large number of numerical simulations of decaying (Cho and Polvani 1996) and forced turbulence (Williams 1978; Vallis and Maltrud 1993; Galperin et al. 2006).

Regarding the spontaneous formation of jets, there are several theoretical approaches discussed in the literature. These include turbulent cascades, modulational instability, mixing of potential vorticity, and statistical theories. According to the turbulent cascade approach, nonlinear eddy–eddy interactions, which are local in

wavenumber space, lead to an inverse energy cascade that is “arrested” by weakly interacting Rossby waves when it reaches the Rhines scale (Rhines 1975). Because of differential rotation, the “arrest” is anisotropic in wavenumber space and allows a further upscale energy transfer to the zonal flow through a narrow region in wavenumber space (Vallis and Maltrud 1993; Nazarenko and Quinn 2009). However, observations of the atmospheric midlatitude jet (Shepherd 1987b) and numerical analysis of simulations (Nozawa and Yoden 1997; Huang and Robinson 1998) showed that the jets are maintained by spectrally nonlocal interactions rather than by a spectrally local cascade.

Modulational instability depends on eddy–eddy interactions that are nonlocal in wavenumber space: a primary meridional Rossby wave interacts with the zonal mean flow and another Rossby wave and transfers its energy directly to the zonal jet bypassing the turbulent cascade (Lorenz 1972; Gill 1974; Manfroi and Young 1999; Connaughton et al. 2010). The drawback in this approach is that it requires a constant source of finite-amplitude meridional waves. Baroclinic instability can provide such a source, but its application to almost barotropic flows (as, for example, in the Jovian atmosphere) is questionable.

---

*Corresponding author address:* Nikolaos A. Bakas, National and Kapodistrian University of Athens, Build. IV, office 34, Panepistimiopolis, Zografos, Athens 15678, Greece.  
E-mail: nikos.bakas@gmail.com

Formation of jets through potential vorticity (PV) mixing envisions that Rossby wave breaking produces turbulent mixing of potential vorticity. The mixing homogenizes vorticity in localized regions, forming staircases in the vorticity gradient that correspond to mean zonal jets (Dritchel and McIntyre 2008; Dunkerton and Scott 2008). While PV staircases have been illustrated in numerical simulations and observations [see Scott and Dritchel (2012) and references therein], there are many cases in which mixing is insufficient to produce a perfect staircase structure, yet robust jets are maintained by the eddies.

Statistical equilibrium theory has also been advanced to explain emergence and formation of jets. This theory is based on the principle that turbulence tends to produce configurations that maximize entropy while conserving both energy and enstrophy. These maximum entropy configurations in two-dimensional flows assume the form of zonal jets or large-scale vortices [see review by Bouchet and Venaille (2012)]. However, the relevance of these results in planetary flows that are strongly forced and dissipated and therefore out of equilibrium remains to be shown.

Nonequilibrium statistical theories that can address such regimes are the stochastic structural stability theory (SSST; Farrell and Ioannou 2003, 2007) or the closely related second-order cumulant expansion theory (CE2) (Marston et al. 2008; Marston 2012). These theories depend on a second-order closure of the dynamics and therefore account explicitly only for the quasi-linear wave–mean flow interactions. According to SSST, an infinitesimal mean flow perturbation can organize the turbulent small-scale eddies in a way that the eddy fluxes reinforce the mean flow to produce a turbulence–mean flow cooperative instability leading to the emergence of exponentially growing jets. While the structure and the properties of the instability were studied in stochastically forced–dissipative barotropic flows (Farrell and Ioannou 2007; Bakas and Ioannou 2011; Srinivasan and Young 2012), the mechanism for the formation of jets needs to be elucidated. In this work, we undertake this task and systematically investigate the eddy–mean flow instability and its dependence on the forcing structure.

SSST has three building blocks. The first is that the eddy statistics can be obtained by retaining only the wave–mean flow interactions in the eddy dynamics. The second building block is to form, based on the quasi-linear approximation, the deterministic dynamics for the joint evolution of the eddy statistics and the mean flow. Since the eddy–eddy nonlinearity is not retained explicitly, this is equivalent to a second-order closure of the eddy cumulant expansion. The third building block is to parameterize the eddy–eddy nonlinearity as stochastic

forcing and enhanced dissipation (Farrell and Ioannou 1993a; DelSole 2004). The resulting nonlinear SSST system governing the evolution of the mean flow and the eddy statistics produces bounded trajectories that are attracted to fixed points, representing steady mean flows in statistical equilibrium with their mean eddy forcing and dissipation, limit cycles, or chaotic attractors. Despite the neglect of the eddy–eddy nonlinearity, the jets in quasi-linear or SSST models were found to be in close correspondence to the jets obtained by fully nonlinear integrations in barotropic (Srinivasan and Young 2012; Constantinou et al. 2013, manuscript submitted to *J. Atmos. Sci.*), quasigeostrophic (DelSole and Farrell 1996; DelSole 1996, 2004), and primitive equations models (O’Gorman and Schneider 2007). As a result, SSST presents an accurate turbulence closure with which we can pursue theoretical study of the formation and maintenance of jets in turbulence.

Comparison of the stability analysis of the SSST system with nonlinear simulations have shown that the emergent jets can be traced to the most unstable mode of the SSST system (Srinivasan and Young 2012; Constantinou et al. 2013, manuscript submitted to *J. Atmos. Sci.*). Finite-amplitude jets can be maintained by shear straining of the turbulent field (Huang and Robinson 1998) and shear straining of the eddies by the emergent mean flow could be similarly proposed to be also responsible for the jet-forming instability. However, the shear straining mechanism was shown to produce upgradient momentum fluxes when the dissipation is weak and the eddies have time to shear over. Given that for an emerging jet the characteristic shear time scale is necessarily infinitely longer than the dissipation time scale, it needs to be shown that shear straining can produce upgradient momentum fluxes in this case as well. In addition, previous studies have shown that shearing of isotropic eddies on an infinite domain and in the absence of dissipation and  $\beta$  does not produce any net momentum fluxes (Shepherd 1985; Farrell 1987; Holloway 2010). This point was also raised by Srinivasan and Young (2012) in their study of jet formation in a barotropic  $\beta$ -plane doubly periodic channel within the framework of SSST. They have shown that isotropically forced eddies evolving in a  $\beta$ -plane constant shear flow on an infinite domain do not produce any net momentum fluxes, yet they found structural instability and jet emergence in both an infinite and a doubly periodic channel. One possibility is that finite domain effects break the symmetry of isotropy and can lead to upgradient fluxes (Shepherd 1987a; Cummins and Holloway 2010). However, since the results in the infinite domain and the periodic channel agree in Srinivasan and Young (2012) another mechanism should

be responsible for producing the upgradient fluxes in these simulations.

In this work we identify physical mechanisms that promote or obstruct jet formation. We show that shear straining of small-scale eddies by the local shear of an infinitesimal sinusoidal mean flow, as described by Orr dynamics in a  $\beta$  plane, intensifies in general the jet. We show that a mean flow velocity perturbation interacting with an anisotropic eddy field induces momentum fluxes that reinforce the mean flow, exactly as if the mean flow were acted by a negative viscosity. We also show that a mean flow velocity perturbation interacting with an isotropic eddy field induces upgradient momentum fluxes caused by changes in the propagation of the eddies that act as a negative hyperviscosity on the mean flow.

## 2. Statistical wave–mean flow barotropic dynamics

Consider a forced, barotropic flow on an infinite  $\beta$  plane. Relative vorticity  $q(x, y, t)$  evolves according to

$$\partial_t q + J(\psi, q) + \beta \partial_x \psi = -r q + f_e, \tag{1}$$

where  $J(A, B) = A_x B_y - A_y B_x$ ,  $\psi$  is the streamfunction, and  $r$  is the coefficient of linear dissipation that typically parameterizes Ekman drag. The forcing term  $f_e$  arises from processes that are missing from the barotropic dynamics (e.g., cascade of energy from baroclinic to barotropic eddies, or small-scale convection) and is typically taken as a spatially homogeneous, random stirring. We decompose the fields into their zonal mean component, denoted with capital letters, and perturbations from this mean, denoted with primes. Under this decomposition and assuming a vanishing external excitation for the zonal mean flow, (1) is split into two equations governing the evolution of the perturbations  $q'$  and the zonal component of the zonal mean velocity  $U$ :

$$(\partial_t + U \partial_x) q' + (\beta - U_{yy}) \partial_x \psi' = -r q' + \underbrace{f_e + f_{nl}}_f, \tag{2}$$

$$\partial_t U = -\partial_y \overline{u'v'} - r U, \tag{3}$$

where  $(u', v') = (-\partial_y \psi', \partial_x \psi')$  denote the zonal and meridional eddy velocities, respectively. The overbar denotes a zonal average and  $f_{nl} = J(\psi', q') - J(\psi, q')$  is the nonlinear term representing the perturbation–perturbation interactions. Previous studies have shown that it suffices to retain only the interaction between the large-scale flow and the perturbations to obtain accurate statistics of the eddies as well as realistic mean flow statistical equilibria (Farrell and Ioannou 1993a; DelSole

and Farrell 1996; DelSole 1999, 2004; O’Gorman and Schneider 2007; Marston 2010). The forcing term  $f_{nl}$  can be either neglected (Marston 2012) or, in order to parameterize nonlinear cascading processes, it can be represented as a random broadband forcing augmented with an additional effective eddy damping to conserve energy (DelSole 2001; Farrell and Ioannou 2009). In this work, both forcing terms  $f = f_e + f_{nl}$  will be represented as a stochastic excitation without distinction.

We now derive a system of equations governing the evolution of the eddy statistics and the mean flow using the continuous formulation of Srinivasan and Young (2012) rather than the matrix formulation of Farrell and Ioannou (2003). The correspondence between the two formulations is discussed in appendix A. We first derive an equation for the evolution of two-point eddy correlation functions, and then relate the eddy momentum fluxes  $\overline{u'v'}$  that drive the mean flow to these functions. We start by assuming that the stochastic forcing has a two-point, two-time correlation function of the form

$$\langle f(x_1, y_1, t_1) f(x_2, y_2, t_2) \rangle = \delta(t_2 - t_1) Q(x_1, x_2, y_1, y_2), \tag{4}$$

where the angle brackets denote an ensemble average. The forcing is assumed to be spatially homogeneous; that is,  $Q$  is a function of the differences  $\tilde{x} = x_1 - x_2$  and  $\tilde{y} = y_1 - y_2$ . We use the shorthand  $a_i = a_i(\mathbf{x}_i, t)$ , with  $i = 1, 2$  to refer to the value of the variable  $a$  at the points  $\mathbf{x}_i = (x_i, y_i)$ . To calculate the equation for the evolution of the vorticity covariance function  $C(\mathbf{x}_1, \mathbf{x}_2, t) = \langle q'_1 q'_2 \rangle$ , we write (2) in the following compact form:

$$\partial_t q'_i = A_i q'_i + f_i, \tag{5}$$

where

$$A_i = -U_i \partial_{x_i} - (\beta - U_{y_i y_i}) \Delta_i^{-1} \partial_{x_i} - r \tag{6}$$

is the dynamical operator evaluated at points  $\mathbf{x}_i$  and  $\Delta_i^{-1}$  is the inverse Laplacian. The streamfunction, in terms of this operator, is  $\psi = \Delta^{-1} q$  and consequently the velocities are  $u = -\partial_y \Delta^{-1} q$  and  $v = \partial_x \Delta^{-1} q$ . Multiplying (5) for  $\partial_t q'_1$  by  $q'_2$  and (5) for  $\partial_t q'_2$  by  $q'_1$ , adding the two equations, and taking the ensemble average we obtain

$$\partial_t C = (A_1 + A_2) C + \langle f_1 q'_2 + f_2 q'_1 \rangle. \tag{7}$$

Note that  $A_1$  and  $A_2$  commute, and that  $C$  is a function of  $x_1 - x_2$ , since  $A_1, A_2$ , and  $Q$  are all homogeneous in  $x$ . Note also that for delta correlated forcing, the ensemble average enstrophy injection rate,  $\langle f_1 q'_2 + f_2 q'_1 \rangle = \langle f_1 f_2 \rangle \equiv Q$ , is independent of the state of the system and (7) becomes

$$\partial_t C = (A_1 + A_2)C + Q. \tag{8}$$

The momentum fluxes can be written in terms of the vorticity covariance function as

$$\langle u'v' \rangle = \langle u'_1 v'_2 \rangle_{\mathbf{x}_1 = \mathbf{x}_2} = -(\partial_{x_2 y_1}^2 \Delta_1^{-1} \Delta_2^{-1} C)_{\mathbf{x}_1 = \mathbf{x}_2}. \tag{9}$$

The subscript  $\mathbf{x}_1 = \mathbf{x}_2$  means that the expression in parenthesis, which is a function of the two points  $\mathbf{x}_1$  and  $\mathbf{x}_2$ , is calculated at the same point. We make the ergodic assumption that the ensemble average is equal to the zonal average; that is, we assume that  $u'v' = \langle u'v' \rangle$ . Then (3) becomes

$$\frac{\partial U}{\partial t} = (\partial_{x_2 y_1 y_2}^3 \Delta_1^{-1} \Delta_2^{-1} C)_{\mathbf{x}_1 = \mathbf{x}_2} - rU. \tag{10}$$

With this assumption, (8) and (10) form a closed deterministic system for the evolution of  $C$  and  $U$ . This coupled system constitutes a second-order closure for the dynamics and is the basis of the SSST.

To solve (8) and (10), Srinivasan and Young (2012) introduce the collective coordinates  $\tilde{x} = x_1 - x_2$ ,  $\tilde{y} = y_1 - y_2$ , and  $\bar{y} = (1/2)(y_1 + y_2)$ . Assuming homogeneity only in  $x$  the Laplacian takes the form  $\Delta_i = \tilde{\Delta} + (-1)^{i+1} \partial_{\tilde{y}}^2 + (1/4) \partial_{\tilde{y}}^2$ , with  $\tilde{\Delta} = \partial_{\tilde{x}}^2 + \partial_{\tilde{y}}^2$ . By introducing the streamfunction covariance,  $\Psi(\tilde{x}, \tilde{y}, \bar{y}) = \langle \psi'_1 \psi'_2 \rangle$ , which is related to  $C$  by

$$\begin{aligned} C &= \langle \Delta_1 \psi'_1 \Delta_2 \psi'_2 \rangle = \Delta_1 \Delta_2 \Psi \\ &= \tilde{\Delta}^2 \Psi + \frac{1}{2} (\partial_{\tilde{x}}^2 - \partial_{\tilde{y}}^2) \partial_{\tilde{y}}^2 \Psi + \frac{1}{16} \partial_{\tilde{y}}^4 \Psi, \end{aligned} \tag{11}$$

the SSST system (8) and (10) takes the form

$$\begin{aligned} \partial_t C + (U_1 - U_2) \partial_{\tilde{x}} C - (U_1'' - U_2'') \left( \tilde{\Delta} + \frac{1}{4} \partial_{\tilde{y}}^2 \right) \partial_{\tilde{x}} \Psi \\ - (2\beta - U_1'' - U_2'') \partial_{\tilde{x} \tilde{y}}^3 \Psi + 2rC = Q, \end{aligned} \tag{12}$$

$$\partial_t U = -\partial_{\tilde{x} \tilde{y}}^3 \Psi|_{\tilde{x} = \tilde{y} = 0} - rU. \tag{13}$$

Equations (12) and (13) may have equilibria, with mean flow  $U^E$  and covariance  $C^E$ . For a spatially homogeneous forcing  $Q$  we always have the equilibrium

$$U^E = 0, \quad C^E = \frac{Q}{2r}. \tag{14}$$

However, this equilibrium is unstable when a critical threshold forcing amplitude is exceeded and the flow transitions to a new state in which the homogeneity is broken with the emergence of zonal jets (Farrell and Ioannou 2007; Bakas and Ioannou 2011; Srinivasan and

Young 2012). These jets are examples of new equilibria that emerge in SSST dynamics. This phenomenon of spontaneous jet emergence has been documented in simulations and experiments of  $\beta$ -plane turbulence (Vallis and Maltrud 1993; Read et al. 2007; Scott and Polvani 2008). In the context of SSST, this phenomenon can be addressed by performing stability analysis of the equilibrium  $U^E$ ,  $C^E$  using the SSST equations. A small perturbation mean flow  $\delta U$  and perturbation covariances  $\delta C$  and  $\delta \Psi$  about this equilibrium obey the linear equations

$$\begin{aligned} \partial_t \delta C &= -(\delta U_1 - \delta U_2) \partial_{\tilde{x}} C^E \\ &\quad + (\delta U_1'' - \delta U_2'') \tilde{\Delta} \partial_{\tilde{x}} \Psi^E \\ &\quad + 2\beta \partial_{\tilde{x} \tilde{y}}^3 \delta \Psi - 2r \delta C \end{aligned} \tag{15}$$

$$\partial_t \delta U = -\partial_{\tilde{x} \tilde{y}}^3 \delta \Psi|_{\tilde{x} = \tilde{y} = 0} - r \delta U. \tag{16}$$

The stability of the equilibrium  $U^E$  and  $C^E$  is consequently reduced to the eigenanalysis of the linearized equations in (15) and (16). Eigenanalysis of (15) and (16) reveals that the homogeneous equilibrium is unstable when the forcing amplitude exceeds a threshold that depends on the damping and the forcing structure. A jet-emerging instability occurs if a seed mean flow organizes the eddies so that the eddy fluxes reinforce it, producing a positive feedback that results in the exponential growth of the jet. This eddy-mean flow feedback process is therefore crucial for the instability, and will be studied in this work in detail.

### 3. Response of the eddy fluxes to mean flow perturbations

In this section we investigate the effect of the momentum fluxes that arise when the statistical equilibrium in (14) is perturbed by an infinitesimal mean flow  $\delta U$  in order to illuminate the nature of the structural instability leading to jet formation. The perturbation in vorticity covariance  $\delta C$  that is induced by  $\delta U$  can be estimated immediately by assuming that the system (15) and (16) is very close to the stability boundary, so that the growth rate is small. We choose this adiabatic limit because it was shown in Bakas and Ioannou (2011) that a necessary condition for structural instability in the case of jet formation is the existence of upgradient momentum and vorticity fluxes in this limit. In this case the mean flow evolves slowly enough that it remains in equilibrium with the eddy covariance. If the marginally unstable state has eigenvalues with zero imaginary part, then  $d\delta C/dt \simeq 0$ , and the streamfunction perturbation covariance function  $\delta \Psi$  obtained from (15) in this limit is

$$\delta\Psi = \underbrace{P^{-1}(\delta U_1 - \delta U_2)\partial_x C^E}_{\delta\Psi^{ad}} - \underbrace{P^{-1}(\delta U_1'' - \delta U_2'')\tilde{\Delta}\partial_x \Psi^E}_{\delta\Psi^{cu}}, \tag{17}$$

where

$$P = 2\beta\partial_{\tilde{x}\tilde{y}}^3 - 2r\left[\tilde{\Delta}^2 + \frac{1}{2}(\partial_{\tilde{x}}^2 - \partial_{\tilde{y}}^2)\partial_{\tilde{y}}^2 + \frac{1}{16}\partial_{\tilde{y}}^4\right], \tag{18}$$

and  $C^E = \tilde{\Delta}^2\Psi^E$ . The separation of  $\delta\Psi$  into two parts,  $\delta\Psi^{ad}$  and  $\delta\Psi^{cu}$ , is instructive because it isolates two physical processes that contribute to the perturbation covariance: advection of the eddy vorticity (the equilibrium vorticity covariance) by the mean flow perturbation and advection of the perturbed mean flow vorticity  $-\delta U'$  by the eddies. We can thus calculate distinct momentum fluxes originating from these two processes, yielding the total perturbation momentum flux

$$\overline{\delta u'v'}(\tilde{y}) = \partial_{\tilde{x}\tilde{y}}\delta\Psi|_{\tilde{x}=\tilde{y}=0} = \overline{\delta u'v'}^{ad} + \overline{\delta u'v'}^{cu}.$$

The mean flow eigenfunctions of (15) and (16) are harmonic functions  $\delta U_n = \sin(ny)$ , which are indexed by the meridional wavenumber of the mean flow  $n$  (which is a continuous variable for the infinite domain). To calculate the momentum fluxes that result from (17) for a mean flow perturbation of the form  $\delta U = \sin(ny)$  that explicitly and clearly illustrates the behavior of the eddy fluxes, we consider the limit in which the scale of the mean flow  $1/n$  is much larger than the scale of the forcing  $L_f$  so that  $\tilde{n} = nL_f \ll 1$ , and the propagation time scale  $1/\beta L_f$  is at most of the same order as the dissipation time scale  $1/r$ , so that  $\beta L_f \tilde{n} \ll r$ .<sup>1</sup> In this limit the momentum fluxes are approximately given by

$$\overline{\delta u'u'}^{ad} = \frac{n \cos(n\tilde{y})}{8\pi r^2} \left[ A_S - A_\beta \frac{\beta^2 L_f^2}{r^2} (nL_f)^2 - A_C (nL_f)^2 \right] + O[(nL_f)^5] \tag{19}$$

$$\overline{\delta u'v'}^{cu} = -\frac{n \cos(n\tilde{y})}{8\pi r^2} A_P (nL_f)^2 + O[(nL_f)^5], \tag{20}$$

where  $A_S, A_\beta, A_C,$  and  $A_P$  are coefficients that depend on the spectral characteristics of the forcing and are given by (B11) and (B12) (cf. appendix B). The same

result is also obtained if we assume that the eddies evolve in a slowly varying flow according to the local shear and according to the local mean vorticity gradient (cf. appendix B). This shows that in the limit of  $\tilde{n} \ll 1$  and  $\beta L_f \tilde{n} \ll r$ , the eddies evolve according to the local dynamics—an observation that will be utilized in the next section.

We calculate  $A_S, A_\beta, A_C,$  and  $A_P$  for two cases of forcing. We first treat the case of the isotropic forcing considered by Srinivasan and Young (2012):

$$Q(\tilde{x}, \tilde{y}) = K_f J_0 \left( K_f \sqrt{\tilde{x}^2 + \tilde{y}^2} \right), \tag{21}$$

where  $J_0$  is the zeroth-order Bessel function. The representation of this isotropic forcing in wavenumber space is a delta function ring of radius  $K_f$ , for which  $L_f = 1/K_f$ . This isotropic forcing has been typically used in studies of barotropic turbulence and is thought to roughly represent convective forcing at scale  $L_f$  (Scott and Polvani 2008). For this forcing, all coefficients  $A_S, A_C,$  and  $A_P$  are exactly zero and the only nonzero contribution to the momentum fluxes results from  $A_\beta$  (cf. appendix B). The leading-order contributions are

$$\overline{\delta u'v'}^{ad} = \frac{3\beta^2 n^3 \cos(n\tilde{y})}{128K_f^5 r^4} + O[(nL_f)^5], \tag{22}$$

while  $\overline{\delta u'v'}^{cu} = O[(nL_f)^5]$ . The accuracy of these limiting expressions is very good. This is shown in Fig. 1a where the approximate solution is compared to the results from numerical integration of the exact expression given by (B8) for Earthlike parameter values  $\tilde{n} = 0.25$  and  $\beta L_f \tilde{n}/r = 0.6$ . The momentum fluxes originate in this case from the advection of the eddy vorticity and are proportional to the third derivative of  $\delta U$  resulting in a hyperviscous momentum flux divergence that tends to reinforce the mean flow and is therefore destabilizing:

$$-\partial_{\tilde{y}}\overline{\delta u'v'} = \frac{3\beta^2}{128K_f^5 r^4} \frac{d^4\delta U(\tilde{y})}{d\tilde{y}^4}. \tag{23}$$

We thus recover the result in Srinivasan and Young (2012), that the structural instability for an isotropic forcing is of the negative hyperviscosity type.

We now treat the case of an anisotropic forcing with a spatial covariance in the form

$$Q(\tilde{x}, \tilde{y}) = a_{k_f} \cos(k_f \tilde{x}) e^{-\tilde{y}^2/2\delta^2}, \tag{24}$$

which was analytically investigated by Bakas and Ioannou (2011). This covariance, which preferentially excites waves with zero meridional wavenumber, represents

<sup>1</sup> In Earth's atmosphere, the size of the eddies and the jet are about  $10^3$  km and  $4 \times 10^3$  km, respectively, and the eddy dissipation time scale is about 2 days, so that  $\tilde{n} = 0.25$  and  $\beta L_f \tilde{n}/r \sim 0.6$ .

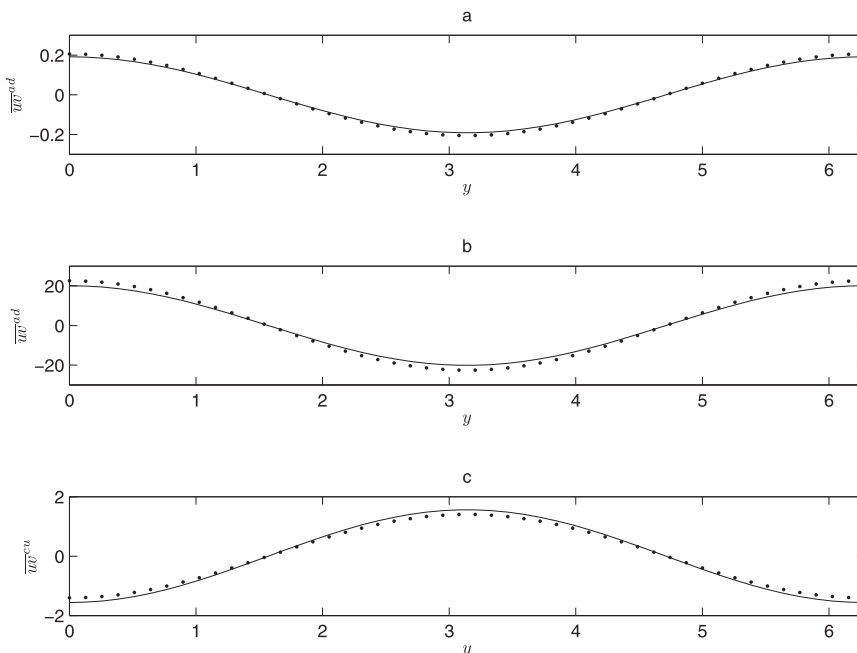


FIG. 1. Quasi-static estimation of the perturbation momentum fluxes that arise when a mean flow perturbation  $\delta U = \sin(y)$  is introduced in a homogeneous turbulent medium at equilibrium. Dots represent the fluxes obtained without approximation from (B8). (a) The flow is stochastically excited with isotropic ring forcing (21) at wavenumber  $K_f = 10$ . The solid line represents the fluxes as calculated by the approximate expression (22). (b),(c) The flow is stochastically excited with anisotropic forcing (24), for which  $k_f = 10$  and  $\delta = 2$ . In (b) the solid line is the fluxes  $\delta u'v'^{ad}$  that arise from advection by  $\delta U$  of the equilibrium eddy vorticity covariance as approximated by (26). In (c) the solid line is the fluxes  $\delta u'v'^{cu}$  that arise from conservative redistribution of the perturbation mean flow vorticity by the equilibrium eddy field, as approximated by (26). In (b) and (c), the fluxes are dominated by the  $A_S$  and  $A_P$  terms in (25) and (26), respectively, while all other terms are negligible and are not shown. In all panels, the damping coefficient is  $r = 0.1$  and  $\beta = 1$ , so that  $\tilde{n} = 0.1$  and  $\beta L_f \tilde{n}/r = 0.1$  and in (b) and (c) the energy input rate is  $\sigma = 1$ .

the forcing of the barotropic flow by the most unstable baroclinic wave, which has zero meridional wavenumber and was shown in previous studies to play an important role in the generation of barotropic jets from an unstable baroclinic shear flow (Berloff et al. 2009a,b). To obtain correspondence with the results of Bakas and Ioannou (2011), we follow the same forcing normalization. That is, we choose the amplitude  $a_{k_f}$  so that the energy density of the forcing per unit of time is a fraction  $\sigma$  of the energy density in a constant flow of unit velocity. In this case, all the coefficients  $A_S, A_C, A_P,$  and  $A_\beta$  are nonzero and the momentum fluxes for a zonally confined forcing ( $k_f \delta \gg 1$ ) are to leading order given by<sup>2</sup>

$$\begin{aligned} \overline{\delta u'v'^{ad}} = & \frac{\sigma n \cos(n\bar{y})}{4r^2} - \frac{3\sigma\beta^2 n^3 \cos(n\bar{y})}{4k_f^6 \delta^2 r^4} - \frac{\sigma n^3 \cos(n\bar{y})}{4k_f^2 r^2} \\ & + O[(nL_f)^5] \end{aligned} \tag{25}$$

$$\overline{\delta u'v'^{cu}} = -\frac{\sigma n^3 \cos(n\bar{y})}{4k_f^2 r^2} + O[(nL_f)^5]. \tag{26}$$

The accuracy of (25) and (26), is shown in Figs. 1b and 1c where the approximate solution is compared to the results from numerical integration of (B8).

In this case, both the advection of the eddy vorticity and the advection of the mean vorticity by the eddies contribute to the momentum fluxes. Shearing of the eddies results, to leading order, in fluxes that are proportional to the shear and to a destabilizing, anti-viscous momentum flux divergence equivalent of negative viscosity

<sup>2</sup> Similar results are also obtained in the opposite limit of a meridionally confined forcing ( $k_f \delta \ll 1$ ). The only exception is the limiting case of an uncorrelated forcing ( $\delta \rightarrow 0$ ), for which the only nonzero coefficient is  $A_P$  leading to downgradient hyperdiffusive fluxes (cf. appendix B).

$$-\partial_{\bar{y}}\delta\overline{u'v'}^{\text{ad}} = -\frac{\sigma}{4r^2}\frac{d^2\delta U(\bar{y})}{d\bar{y}^2}, \quad (27)$$

recovering the result of Bakas and Ioannou (2011). Note that these fluxes are, to leading order, independent of  $\beta$ . This implies that there is a tendency to form jets also in the absence of  $\beta$  as seen, for example, in numerical simulations (Kramer et al. 2008; Bouchet and Simonnet 2009). The other terms in (25) (including the one that is destabilizing for isotropic forcing) act as hyperviscosity and oppose jet formation but are subdominant.

Advection of the perturbed mean flow vorticity by the eddies results in the stabilizing hyperviscous flux divergence:

$$-\partial_{\bar{y}}\delta\overline{u'v'}^{\text{cu}} = -\frac{\sigma}{4k_f^2r^2}\frac{d^4\delta U(\bar{y})}{d\bar{y}^4}. \quad (28)$$

This term is subdominant (of order  $\tilde{n}^2$ ) compared to (27) for  $\tilde{n} \ll 1$ , but it dominates for  $\tilde{n} \gg 1$  and determines the high zonal wavenumber cutoff of the structural instability (Bakas and Ioannou 2011). While advection of the perturbed mean flow vorticity by the eddies is stabilizing in this case, it can be jet forming in the presence of topography. To illustrate this, consider forced turbulence in a stratified flow with a Rossby radius of deformation  $R_d$ , above topography of small elevation  $\eta$ , and consider for simplicity topography consisting of zonal ridges (i.e., take  $\eta$  to be zonally invariant). Then (28) implies that the vorticity fluxes due to advection of the mean potential vorticity  $q^m = \beta y + \eta/R_d^2$  by the eddies will be proportional to  $q_{yyy}^m = \eta_{yyy}/R_d^2$ . As a result, jets will tend to form in regions where the absolute value of the potential vorticity gradient is maximum in agreement with numerical simulations (Thompson 2010). It is clear from this analysis that the structural instability that results from the isotropic and the anisotropic forcing used in the studies of Srinivasan and Young (2012) and Farrell and Ioannou (2003, 2007) will have markedly different dependence on parameters. In the next section we will investigate the underlying physical processes that produce these fluxes.

#### 4. Analysis of the dynamics underlying the eddy fluxes

In this section we study the dynamics producing the diffusive and hyperdiffusive eddy fluxes that lead to jet formation. We show that shear straining of the eddies by the local shear is the dominant destabilizing process. We assume again that near the stability boundary  $d\delta C/dt \simeq 0$ . The perturbation momentum fluxes induced

by a sinusoidal mean flow perturbation  $\delta U = \sin(ny)$  can be alternatively calculated from

$$\delta\langle u'v' \rangle = \frac{1}{2\pi} \int_{-\infty}^{\infty} \int_{-\infty}^{\infty} \overline{u'v'}_{\infty} d\xi dk, \quad (29)$$

where

$$\overline{u'v'}_{\infty} = \int_0^{\infty} \overline{u'v'}(t) dt, \quad (30)$$

$\overline{u'v'}(t)$  is the momentum flux at time  $t$  produced by the initial perturbation

$$G(x, y - \xi) = \frac{e^{ikx}}{\sqrt{2\pi}} \int_{-\infty}^{\infty} \sqrt{\hat{Q}(k, l)} e^{il(y-\xi)} dl, \quad (31)$$

which is localized at latitude  $\xi$  and  $\hat{Q}(k, l)$  is the Fourier amplitude of the spatially homogeneous forcing covariance  $Q(\bar{x}, \bar{y})$  (cf. appendix C). Equation (29) expresses the physically expected result that the ensemble mean induced momentum flux is equal to the integral over time and over all zonal wavenumbers of the responses to all point excitations in the  $y$  direction. We will now show that  $G$  takes the form of a wavepacket for both the isotropic and anisotropic forcing studied in the previous section.

Consider first the isotropic ring forcing

$$\hat{Q}(k, l) = \frac{\Theta(\Delta K - |\sqrt{k^2 + l^2} - K_f|)}{2\Delta K}, \quad (32)$$

where  $\Theta$  is the step function [ $\Theta(x) = 0$  when  $x < 0$  and  $\Theta(x) = 1$  when  $x \geq 0$ ]. When the width of the ring  $\Delta K$  around wavenumber  $K_f$  goes to zero, this forcing approaches the narrow band ring forcing in (21) treated in section 3. For this forcing,  $G$  has the wavepacket form (cf. appendix C)

$$G(k, y - \xi) = B(k)h(y - \xi)e^{ikx + il_0(y-\xi)}, \quad (33)$$

with

$$B(k) = \frac{\sqrt{\Delta K}K_f}{\pi^{1/4}\sqrt{K_f^2 - k^2}}\Theta(K_f - |k|)$$

$$h(y) = e^{-y^2\delta^2/2}, \quad l_0 = \sqrt{K_f^2 - k^2}, \quad (34)$$

and  $\delta = K_f\Delta K/\sqrt{K_f^2 - k^2}$ . The function  $G(k, y - \xi)$  consists of a carrier wave with wavenumbers  $(k, l_0)$  and amplitude  $B(k)$ , which is modulated in the  $y$  direction by the wavepacket envelope  $h(y)$ . Consider now the anisotropic forcing in (24). It is straightforward to show that  $G$  assumes the same form as (33) but with (cf. appendix C)

$$B(k) = \sqrt{\frac{a_{k_l}}{\delta}} (2\pi)^{1/4} [\delta(k - k_f) + \delta(k + k_f)],$$

$$h(y) = e^{-y^2/\delta^2}, \quad l_0 = 0. \quad (35)$$

As a result, the calculation of the ensemble mean momentum fluxes is reduced to calculating the momentum fluxes over the life cycle of wavepackets that are initially at different latitudes and then adding their relative contributions.

We consider, as in the previous section, parameters so that  $nL_f \ll 1$  and  $\beta nL_f^2/r \ll 1$ . In this parameter regime, the eddies are localized compared to the mean flow variations and are dissipated before they propagate away. Because of the small amplitude of  $\delta U$ , the eddies are also dissipated before they shear over. As a result, the waves evolve to a good approximation according to the local dynamics (cf. appendix B). That is, the vorticity of the eddy that is initially localized around  $\xi$  is advected by the local velocity

$$\delta U = \delta U(\xi) + \left(\frac{d\delta U}{dy}\right)_\xi (y - \xi) + \left(\frac{d^2\delta U}{dy^2}\right)_\xi \frac{(y - \xi)^2}{2} + \left(\frac{d^3\delta U}{dy^3}\right)_\xi \frac{(y - \xi)^3}{6} + O(\delta U^{(4)}), \quad (36)$$

and in turn, this eddy advects the local vorticity with gradient

$$Q_y = \beta - \left(\frac{d^2\delta U}{dy^2}\right)_\xi - \left(\frac{d^3\delta U}{dy^3}\right)_\xi (y - \xi) + O(\delta U^{(4)}). \quad (37)$$

When the perturbations are not localized and the slowly varying limit  $nL_f \ll 1$  does not hold, the eddies will be affected by the mean shear and mean  $Q_y$  within their extend. If the propagation time scale is large compared to the dissipation time scale, so that  $\beta nL_f^2/r \ll 1$  does not hold, the eddies will be affected by the mean shear and mean  $Q_y$  within the extent of their propagation.

In section 3, we found that the processes of eddy vorticity advection and advection of the mean flow vorticity by the eddies can be separated, and that their contribution to the total momentum fluxes, denoted as  $\overline{\delta u'v'^{\text{ad}}}$  and  $\overline{\delta u'v'^{\text{cu}}}$ , respectively, is additive. We also found that the solution is linear in the perturbation velocity. As a result, we can calculate  $\overline{\delta u'v'^{\text{ad}}}$  and  $\overline{\delta u'v'^{\text{cu}}}$  by taking each term of (36) and (37) into account separately and then adding the respective contributions. For  $\overline{\delta u'v'^{\text{ad}}}$  we will retain only the local shear, which amounts to calculating the momentum fluxes from an ensemble of wavepackets evolving in

this weak constant shear on a  $\beta$  plane. Similarly, for  $\overline{\delta u'v'^{\text{cu}}}$ , we will retain only the linear change in  $Q_y$  and calculate the momentum fluxes due to advection of the vorticity gradient of the mean flow by the eddies from the evolution of the wavepacket in a fluid with no mean flow but with a vorticity gradient  $Q_y$  given by (37). The ensemble mean momentum fluxes will then be given by (29).

#### a. Shear wave dynamics

Consider first the evolution of an ensemble of wavepackets of the form of (33) in the constant shear flow  $\delta U = \alpha(y - \xi)$ , where  $\alpha = (d\delta U/dy)_\xi$  is the local shear at each latitude  $\xi$  of the emerging flow. The momentum flux of each wavepacket is

$$\overline{u'v'} = -|B|^2 A_M(t) e^{-2rt} |h[y - \xi - \eta(t)]|^2, \quad (38)$$

where  $A_M(t) = kl_l/(k^2 + l_l^2)^2$  is the momentum flux of the carrier wave that determines the amplitude of the fluxes of the wavepacket. The meridional wavenumber,  $l_l = l_0 - \alpha kt$ , decreases with time as the wave is sheared over, while the group velocity of the wavepacket on the  $\beta$  plane,  $c_g = 2\beta A_M$ , is proportional to  $A_M$ . The position of the packet is given by

$$\eta(t) = \frac{\beta}{\alpha} \left( \frac{1}{k^2 + l_l^2} - \frac{1}{k^2 + l_0^2} \right), \quad (39)$$

as was shown by Tung (1983). According to this solution, a wavepacket with phase lines tilted against the shear in an inviscid flow, propagates northward while it gains momentum until  $t = l_0/k\alpha$ , and subsequently propagates southward and asymptotically reaches its critical layer where it surrenders its momentum to the mean flow. On the other hand, a wavepacket with phase lines tilted with the shear propagates southward toward its critical layer while it continuously loses its momentum to the mean flow (Boyd 1983; Tung 1983).

In the presence of strong shear and weak damping, the shear time scale is much smaller than the dissipation time scale and the eddies quickly shear over into the decaying phase that lasts longer than the growing phase. As a result, they decay on average and the mean flow is accelerated by the upgradient momentum fluxes of the shear waves. This is the mechanism for maintaining finite-amplitude jets by an eddy field that is typically referred to as the Orr mechanism (Farrell and Ioannou 1993b; Huang and Robinson 1998). This process ceases to produce upgradient fluxes when the eddy field is isotropic (Shepherd 1985; Farrell 1987).

The limit appropriate for the investigation of the stability of a homogeneous turbulent flow to emerging

infinitesimal mean zonal flows that we address in this work is different, as the shear of the infinitesimal mean flow perturbation is weak and the waves are dissipated before they shear over; that is,  $1/r \ll 1/\alpha$ . In the limit of a weak mean vorticity gradient that we also consider ( $\alpha/r \ll \beta L_f/r \ll 1$ ), the dominant contribution to the time integral in (30) comes from short times, since the perturbation is rapidly attenuated by friction before it propagates or it is sheared over. As a result, the average momentum flux distribution will be determined by two factors: the small change in the amplitude of the fluxes  $A_M$  due to shearing over a dissipation time scale and the small change in the position of the packet that occurs during the same period. For short times ( $\alpha t \ll r t$ ) the variation in the momentum flux amplitude and the location of the wavepacket due to shearing is

$$A_M(t) \simeq A_M(0) + \frac{\alpha k^2(3l_0^2 - k^2)}{(k^2 + l_0^2)^3}t + \dots,$$

$$\eta(t) \simeq c_g(0)t + \frac{\alpha \beta k^2(3l_0^2 - k^2)}{(k^2 + l_0^2)^3}t^2 + \dots \quad (40)$$

Inserting (40) in (38), integrating over time, and keeping the terms that are even in wavenumbers and will have a nonzero contribution when integrated over wavenumbers, we obtain that the integrated over time momentum flux in (30) is given by

$$\begin{aligned} \overline{u'v'}_\infty = & \underbrace{\frac{|B|^2 \beta k^2 l_0^2}{2r^2 (k^2 + l_0^2)^4} \frac{d}{dp} |h(p)|^2 + O(\beta^2)}_{\overline{u'v'_R}} \\ & + \underbrace{\frac{\alpha}{4r^2} \frac{|B|^2 k^2 (k^2 - 3l_0^2)}{(k^2 + l_0^2)^3} |h(p)|^2 + O(\alpha^2)}_{\overline{u'v'_S}} \\ & + \underbrace{\frac{3\alpha\beta^2}{2r^4} \frac{|B|^2 k^4 l_0^2 (k^2 - 3l_0^2)}{(k^2 + l_0^2)^7} \frac{d^2}{dp^2} |h(p)|^2 + O(\alpha\beta^3)}_{\overline{u'v'_\beta}}, \end{aligned} \quad (41)$$

in which  $p = y - \xi$ . The first term,  $\overline{u'v'_R}$ , arises from the momentum fluxes produced by a propagating wavepacket in the absence of shear and does not contribute to the ensemble averaged momentum fluxes when integrated over the initial positions  $\xi$ . The second and third terms arise because of shearing of the wavepacket and correspond to the contribution of the change in the amplitude of the fluxes ( $\overline{u'v'_S}$ ) and the change in the group velocity of the wavepackets ( $\overline{u'v'_\beta}$ ), respectively.

We can qualitatively assess the changes in the distribution of the fluxes obtained in (41) by examining how the amplitude of the fluxes and the group velocity of the packets change as the phase lines of the carrier wave are sheared over. Let  $\theta_t = \arctan(l_t/k)$  be the angle at time  $t$  of the phase lines of the carrier wave of the packet with the  $y$  axis. Figures 2a and 3a illustrate the amplitude of the momentum fluxes  $A_M$  (Fig. 2a) and the group-velocity  $c_g$  (Fig. 3a) at the instance of time at which the phase line orientation is  $\theta_t$ . We first study the effect of the amplitude change by ignoring propagation. Consider a wavepacket starting at some point along the  $\theta_t$  axis with initial angle  $\theta_0 = \arctan(l_0/k)$ . Then the filled circle shown in Fig. 2a gives the initial value of the momentum fluxes. As the packet is sheared over with time,  $\theta_t$  decreases monotonically (owing to the monotonically decreasing  $l_t$ ) and the fluxes at a later time are given by the open circle. Since the wave packet is rapidly dissipated, the integrated momentum fluxes over its lifetime will be given to a good approximation by the change in the fluxes occurring over the dissipation time scale  $1/r$  that is incremental in shear time units. The change in the fluxes will thus be proportional to the local derivative of the curve in Fig. 2a. As a result, the momentum flux of a wavepacket with  $|\theta_0| < \pi/6$  (corresponding to  $k^2 > 3l_0^2$ ) excited in regions II or III will increase within the dissipation time scale.<sup>3</sup> This is also illustrated in Fig. 2b, showing how the momentum flux of a wavepacket with a Gaussian distribution of vorticity with latitude changes as the wave shears over if we ignore propagation. Compared to an unsheared wavepacket, this process leads to the upgradient momentum flux surplus shown in Fig. 2c. The opposite occurs for waves excited in regions I and IV (with  $|\theta_0| < \pi/6$  corresponding to  $k^2 < 3l_0^2$ ) that produce down-gradient fluxes.

We now consider the effect of propagation on the momentum fluxes while ignoring the change in the amplitude. A wavepacket starting in region III will propagate toward the north, as shown by the filled circle in Fig. 3a. Because shearing induces a decrease in the magnitude of the group velocity (open circle in Fig. 3a) the wavepacket will flux its momentum from southern latitudes compared to when it moved in the absence of the shear flow. This is shown in Fig. 3b, illustrating

<sup>3</sup> Note that the angles  $\theta_m = \pm \pi/6$  correspond to the orientations at which a wave with initial vorticity  $B(k)$  maximizes the momentum flux amplitude. If the wave were introduced with initial energy  $E(k)$ , then the momentum fluxes of the carrier wave ignoring dissipation would be given by  $\overline{u'v'_E} = -E(k)kl_l/(k^2 + l_l^2)$  and the orientation maximizing the momentum flux would become  $\theta_m = \pm \pi/4$ .

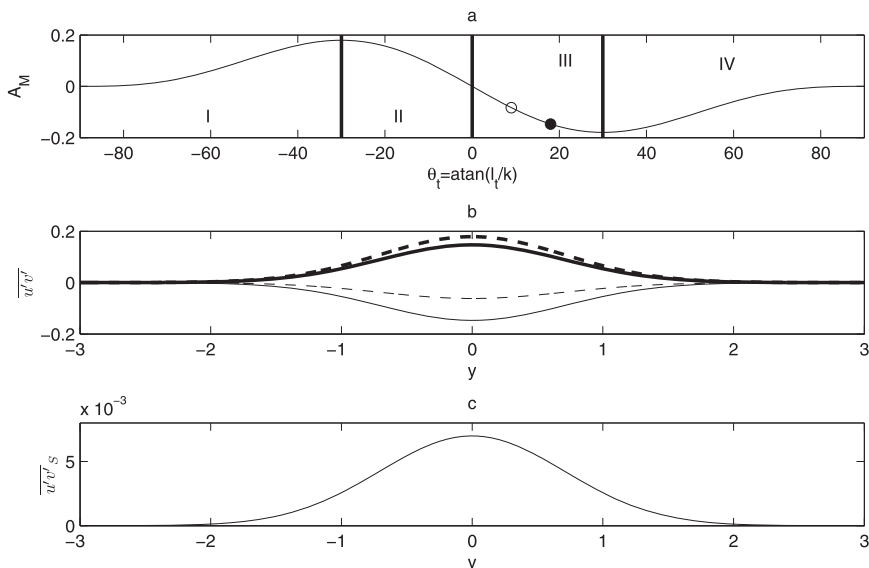


FIG. 2. (a) Momentum fluxes  $A_M(t)$  of wavepackets in a constant shear flow as a function of the angle  $\theta_t = \arctan(l_t/k)$  between the phase lines of the central wave and the  $y$  axis. The wavenumber is given by  $l_t = l_0 - \alpha kt$ , where  $(k, l_0)$  is the initial central wavenumber of the wavepacket and  $\alpha$  is the shear. A wavepacket starting with an inclination at a certain angle  $\theta_0$  (filled circle) will transverse this graph toward the left and its fluxes at a later time will be given by the open circle. The vertical lines separate the regions with  $|\theta_t| < \pi/6$  (II and III) and  $|\theta_t| > \pi/6$  (I and IV). At  $\theta_t = \pm \pi/6$ , the momentum flux has peak magnitude for wavepackets excited with equal vorticity. The central wavenumber of the packet is  $K_f = \sqrt{k^2 + l_0^2} = 1$ . (b) Comparison of the momentum fluxes of an unsheared wavepacket excited in regions II (thick solid line) and III (solid line) to the momentum fluxes of a sheared wavepacket shown by the corresponding dashed lines, when only the change in amplitude is taken into account. A snapshot of the fluxes at  $t = 0.2/r$  is shown. The wavepacket has initial vorticity  $h(y) = e^{-y^2}$ , a central total wavenumber  $K_f = 1$ ,  $|\theta_0| < \pi/10$ , and  $|B| = 1$ . The shear and dissipation time scales are taken as equal ( $\alpha = r = 0.1$ ) for illustration purposes. (c) The difference in momentum fluxes between a sheared and an unsheared wavepacket calculated over their life cycle, when only the effect of the amplitude change  $\overline{u'v'_S}$  is taken into account. The shear is  $\alpha = 10^{-3}$ , while the rest of the parameters are as in (b).

the distribution of momentum fluxes of an unsheared and a sheared perturbation whose amplitudes are constant. Figure 3c plots this difference,  $\overline{u'v'_\beta}$ , and shows that the fluxes are downgradient in this case. The same happens for waves excited in region II, while the waves excited in regions I and IV produce upgradient fluxes.

The net momentum fluxes produced by an ensemble of wavepackets will therefore depend on the spectral characteristics of the forcing that determine the regions (I–IV) in which the forcing has significant power. Consider first the case of the isotropic forcing that results in the wavepackets given by (34). Integrating (41) over all excitation latitudes  $\xi$  and all zonal wavenumbers we obtain

$$\delta \langle u'v' \rangle = \frac{1}{2\pi} \int_{-\infty}^{\infty} \int_{-\infty}^{\infty} \overline{u'v'_R} d\xi dk + \frac{1}{2\pi} \int_{-\infty}^{\infty} \int_{-\infty}^{\infty} \overline{u'v'_S} d\xi dk + \frac{1}{2\pi} \int_{-\infty}^{\infty} \int_{-\infty}^{\infty} \overline{u'v'_\beta} d\xi dk. \tag{42}$$

The first term in (42) is

$$\frac{1}{2\pi} \int_{-\infty}^{\infty} \int_{-\infty}^{\infty} \overline{u'v'_R} d\xi dk = \frac{1}{2\pi} \int_{-\infty}^{\infty} \int_{-\infty}^{\infty} \frac{|B(k)|^2 \beta k^2 l_0^2}{2r^2 (k^2 + l_0^2)^4} \left[ \frac{d}{d\xi} e^{-(y-\xi)^2 \delta(k)^2} \right] d\xi dk = 0. \tag{43}$$

The second term in (42) is

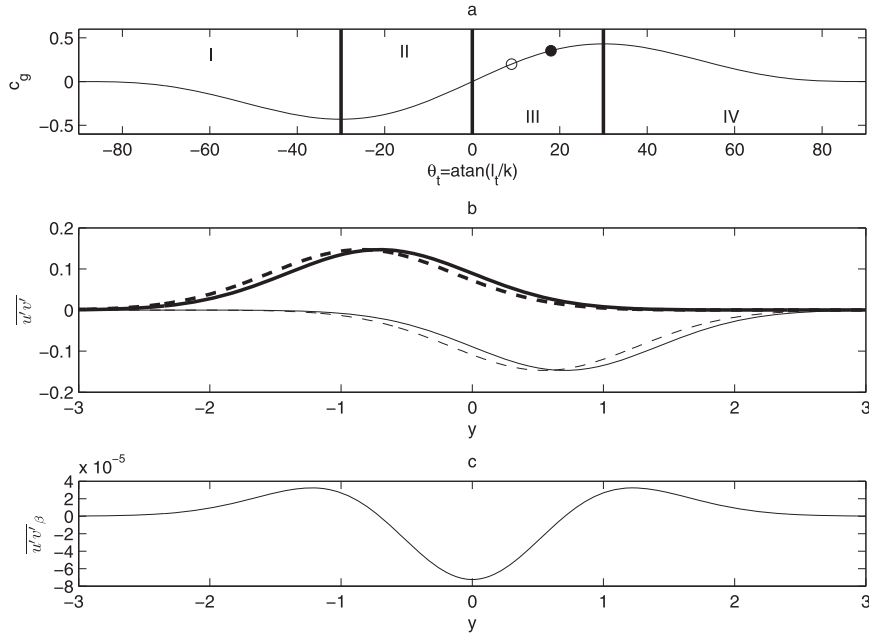


FIG. 3. (a) The group velocity of the wavepackets in a constant shear flow as a function of the angle  $\theta_t = \arctan(l_t/k)$  between the phase lines of the central wave and the  $y$  axis. A wavepacket starting at an angle  $\theta_0$  (filled circle) will transverse this graph toward the left and its group velocity at a later time will be given by the open circle. The regions I–IV are as in Fig. 2a,  $\beta = 0.6$  for illustration purposes, and  $K_f = 1$ . (b) Comparison of the momentum fluxes of an unsheared wavepacket excited in regions II (thick solid line) and III (thin solid line) to the momentum fluxes of a sheared wavepacket shown by the corresponding dashed lines, when only the change in propagation is taken into account. A snapshot of the fluxes at  $t = 0.2/r$  is shown and the rest of the parameters are as in Fig. 2b. (c) The difference in momentum fluxes between a sheared and an unsheared wavepacket calculated over their life cycle, when only the effect of propagation is taken into account. The planetary vorticity gradient is  $\beta = 0.1$  and the rest of the parameters are as in Fig. 2c.

$$\begin{aligned} \frac{1}{2\pi} \int_{-\infty}^{\infty} \int_{-\infty}^{\infty} \overline{u'v'_S} d\xi dk &= \frac{1}{2\pi} \int_{-\infty}^{\infty} \frac{|B(k)|^2 k^2 (k^2 - 3l_0^2)}{4r^2 (k^2 + l_0^2)^3} \left[ \int_{-\infty}^{\infty} \frac{d\delta U}{d\xi} e^{-(y-\xi)^2 \delta(k)^2} d\xi \right] dk \\ &\simeq \frac{\Delta K}{4\pi^{3/2} r^2 K_f^4} \int_{-K_f}^{K_f} \frac{k^2 (4k^2 - 3K_f^2)}{K_f^2 - k^2} \left[ \frac{d\delta U}{dy} \int_{-\infty}^{\infty} e^{-(y-\xi)^2 \delta(k)^2} d\xi \right] dk, \end{aligned} \tag{44}$$

in which we have used the approximation that for a slowly varying flow ( $nL_f \ll 1$ ), the shear  $d\delta U/d\xi$  over the wavepacket envelope  $h = e^{-(y-\xi)^2 \delta(k)^2}$  can be approximated by its value at  $\xi = y$ . The third term in (42) is

$$\begin{aligned} \frac{1}{2\pi} \int_{-\infty}^{\infty} \int_{-\infty}^{\infty} \overline{u'v'_\beta} d\xi dk &= \frac{1}{2\pi} \int_{-\infty}^{\infty} \frac{3\beta^2 |B(k)|^2 k^4 l_0^2 (k^2 - 3l_0^2)}{2r^4 (k^2 + l_0^2)^7} \left\{ \int_{-\infty}^{\infty} \frac{d\delta U}{d\xi} \left[ \frac{d^2}{d\xi^2} e^{-(y-\xi)^2 \delta(k)^2} \right] d\xi \right\} dk \\ &= \frac{3\beta^2 \Delta K}{2\pi^{3/2} r^4 K_f^{12}} \int_{-K_f}^{K_f} k^4 (4k^2 - 3K_f^2) \left[ \int_{-\infty}^{\infty} \frac{d^3 \delta U}{d\xi^3} e^{-(y-\xi)^2 \delta(k)^2} d\xi \right] dk \\ &\simeq \frac{3\beta^2 \Delta K}{2\pi^{3/2} r^4 K_f^{12}} \int_{-K_f}^{K_f} k^4 (4k^2 - 3K_f^2) \left[ \frac{d^3 \delta U}{dy^3} \int_{-\infty}^{\infty} e^{-(y-\xi)^2 \delta(k)^2} d\xi \right] dk, \end{aligned} \tag{45}$$

in which we used the slowly varying approximation as in (44). Consequently (42) becomes

$$\begin{aligned} \delta\langle u'v' \rangle &= \frac{1}{2\pi} \int_{-\infty}^{\infty} \int_{-\infty}^{\infty} \overline{u'v'_S} d\xi dk + \frac{1}{2\pi} \int_{-\infty}^{\infty} \int_{-\infty}^{\infty} \overline{u'v'_\beta} d\xi dk \\ &\simeq \frac{1}{4\pi r^2 K_f^5} \frac{d\delta U}{dy} \int_{-K_f}^{K_f} \frac{k^2(4k^2 - 3K_f^2)}{\sqrt{K_f^2 - k^2}} dk + \frac{3\beta^2}{2\pi K_f^{13}} \frac{d^3\delta U}{dy^3} \int_{-K_f}^{K_f} k^4(4k^2 - 3K_f^2) \sqrt{K_f^2 - k^2} dk \\ &= -\frac{3\beta^2}{64\pi K_f^2 r^4} \frac{d^3\delta U}{dy^3}. \end{aligned} \tag{46}$$

The first integral is the ensemble mean momentum fluxes that result from  $\overline{u'v'_S}$  and are proportional to the shear. This term therefore corresponds to the  $A_S$  term in (19). The net fluxes are shown to be exactly zero for isotropic forcing because the gain in momentum occurring for  $|\theta_0| < \pi/6$  (waves excited in regions II and III) is fully compensated by the loss in momentum for  $|\theta_0| > \pi/6$  (waves excited in regions I and IV). Full compensation occurs because we are equally exciting all possible wave orientations. This exact cancelation is a peculiarity of isotropic forcing in an unbounded domain. A finite domain, as is the case in physically realizable flows, can affect this symmetry and lead to partial cancelation and to upgradient fluxes, as was noted in previous studies (Shepherd 1987a; Cummins and Holloway 2010). In (46), the net momentum fluxes are produced by the  $\overline{u'v'_\beta}$  term and are upgradient for isotropic forcing. The reason is that the loss in momentum occurring for  $|\theta_0| < \pi/6$  is overcompensated by the gain in momentum for  $|\theta_0| > \pi/6$ . The momentum fluxes are hyperdiffusive and the wavepacket analysis reproduces (22) modulo a factor of 2.

Consider now the case of the anisotropic forcing in (24) resulting in wavepackets of the form in (35). Following the same analysis as in (42)–(46), we obtain

$$\begin{aligned} \delta\langle u'v' \rangle &= \frac{1}{2\pi} \int_{-\infty}^{\infty} \int_{-\infty}^{\infty} \overline{u'v'_S} d\xi dk + \frac{1}{2\pi} \int_{-\infty}^{\infty} \int_{-\infty}^{\infty} \overline{u'v'_\beta} d\xi dk \\ &\simeq \frac{\sigma}{4r^2} \frac{d\delta U}{dy} + O(\beta^2). \end{aligned} \tag{47}$$

That is,  $\overline{u'v'_S}$  yields upgradient fluxes because we excite a band of waves mainly in regions II and III (as this forcing is centered at  $l_0 = 0$  in wavenumber space). We have therefore revealed the dynamics underlying the first two terms<sup>4</sup> in (19). In summary, the change in the amplitude of the momentum fluxes caused by shearing

of the eddies leads to upgradient antidiffusive ensemble mean momentum fluxes that reinforce the mean flow except for isotropic forcing in which case it has no effect. The change in the group velocity of the eddies due to shearing leads to hyperdiffusive fluxes with a positive or negative coefficient depending on the characteristics of the forcing.

*b. Dynamics of wave propagation in the presence of a mean vorticity gradient*

We now calculate the momentum fluxes produced by an ensemble of wavepackets propagating in a flow with the linearly varying  $Q_y = \beta - \gamma(y - \xi)$ , with  $d^2\delta U/dy^2|_\xi = 0$  and  $d^3\delta U/dy^3|_\xi = \gamma$ . Under the slowly varying approximation, the wavepacket has a local phase speed  $c = [\beta - \gamma(y - \xi)]/(k^2 + l_0^2)$ . Its phase lines are therefore “sheared” over because of the change in  $Q_y$ , resulting in a decreasing wavenumber

$$l_t \simeq l_0 - \gamma kt/(k^2 + l_0^2). \tag{48}$$

We therefore expect a similar solution for the fluxes as in section 4a. Using ray tracing, it is shown in appendix D that the momentum fluxes for each of the wavepackets are indeed given by the same (38), except that  $l_t$  and  $\eta$  satisfy (D2) in this case. For small times,  $l_t$  satisfies the heuristically derived (48) and the dynamics are homomorphic to the shear wave dynamics described in section 4a.

As in shearing of the wavepacket by the mean flow, the momentum flux distribution produced by this wavepacket over its life cycle will be determined by the small change in the amplitude of the fluxes and the small change in the position of the packet that will occur within a dissipation time scale. In appendix D, it is shown that the momentum fluxes produced by this wavepacket over its life cycle are

$$\overline{u'v'}_\infty = \overline{u'v'}_R + \underbrace{\frac{\gamma}{4r^2} \frac{|B|^2 k^2 (k^2 - 3l_0^2)}{(k^2 + l_0^2)^4} |h(p)|^2}_{\overline{u'v'_p}} + O(\gamma\beta). \tag{49}$$

<sup>4</sup> To investigate the third term, we need to take into account the third derivative of  $\delta U$  in (36). However, since this turns out to be a stabilizing term for the cases considered, we will not pursue this further.

The first term  $\overline{u'v'_R}$  is the same as in (41) and does not contribute to the net ensemble mean momentum fluxes. The second term  $\overline{u'v'_P}$ , which is independent of  $\beta$ , arises solely because of the change in the amplitude of the momentum fluxes. This result can be comprehended qualitatively by examining again Fig. 2a, showing how the momentum fluxes change with  $\theta_t$ . The only difference in this case is the time that it takes for a wave to transverse this graph toward the left, as  $l_t$  decreases monotonically but by a different amount compared to the case in section 4a. However, this difference is not relevant with regard to the momentum flux changes, as we are interested in changes within the dissipation time scale that are infinitesimal compared to the evolution time scale for  $l_t$  [which is  $O(1/\alpha) \gg 1$  in section 4a and  $O(1/\gamma) \gg 1$  here]. As a result, the momentum fluxes of a wavepacket excited in regions II and III will again decrease within the dissipation time scale. This leads to the same flux surplus shown in Fig. 2c when  $\gamma = \alpha$ . However, the amplitude is proportional to the third derivative of the mean flow  $\gamma$ , rather than proportional to the shear, and the momentum fluxes are therefore down-gradient. The opposite occurs for waves excited in regions I and IV, producing upgradient fluxes.

We will now calculate the ensemble average momentum fluxes produced for the cases of isotropic and anisotropic forcing. Following the analysis in (42)–(46), we obtain that for the isotropic forcing in (21)

$$\begin{aligned} \delta\langle u'v' \rangle &= \frac{1}{2\pi} \int_{-\infty}^{\infty} \int_{-\infty}^{\infty} \overline{u'v'_R} d\xi dk + \frac{1}{2\pi} \int_{-\infty}^{\infty} \int_{-\infty}^{\infty} \overline{u'v'_P} d\xi dk \\ &\simeq \frac{1}{4\pi r^2 K_f^2} \frac{d^3 \delta U}{dy^3} \int_{-K_f}^{K_f} \frac{k^2(4k^2 - 3K_f^2)}{\sqrt{K_f^2 - k^2}} dk = 0. \end{aligned} \tag{50}$$

That is, the net momentum fluxes produced are zero, as the loss in momentum occurring for  $|\theta_0| < \pi/6$  is fully compensated by the gain in momentum for  $|\theta_0| > \pi/6$ . For the anisotropic forcing in (24), we obtain

$$\begin{aligned} \delta\langle u'v' \rangle &= \frac{1}{2\pi} \int_{-\infty}^{\infty} \int_{-\infty}^{\infty} \overline{u'v'_R} d\xi dk + \frac{1}{2\pi} \int_{-\infty}^{\infty} \int_{-\infty}^{\infty} \overline{u'v'_P} d\xi dk \\ &\simeq \frac{\sigma}{4k_f^2 r^2} \frac{d^3 \delta U}{dy^3}. \end{aligned} \tag{51}$$

That is, “shearing” of the perturbation due to the meridional variation of  $Q_y$  produces hyperdiffusive fluxes with an amplitude independent of  $\beta$  and therefore corresponds to the  $A_P$  term in (20).

### 5. Conclusions

Large-scale zonal jets are commonly observed to spontaneously emerge in turbulent fluids. The mechanism for jet formation in a barotropic  $\beta$  plane under homogeneous stochastic forcing was examined in this work within a statistical wave–mean flow interaction framework. In this framework, the eddy–eddy nonlinearity is parameterized or ignored. This approximation leads to a deterministic system for the coevolution of the zonal mean jet and the ensemble mean covariance of the perturbation fields. This dynamics is the subject of stochastic structural stability theory (SSST) (Farrell and Ioannou 2003).

We derived in this work the SSST system with the continuous formulation of Srinivasan and Young (2012) and derived the correspondence with the matrix formulation of the same equations. We then discussed the structural stability of a homogeneous equilibrium maintained against dissipation by a spatially homogeneous and delta-correlated-in-time stochastic excitation. It is known that in such flows on a  $\beta$  plane, the homogeneous state is structurally unstable when a critical value of forcing is exceeded and zonal jets emerge. We focused our analysis close to this bifurcation point in order to identify the processes that lead to the emergence of jets. Investigation of the ensemble mean momentum fluxes revealed that the eddy–mean flow dynamics can be split into two distinct processes: advection of the eddy vorticity by the weak mean flow and advection of the vorticity of the mean flow by the eddies. Eddy vorticity advection was found to lead to hyperdiffusive fluxes with a negative diffusion coefficient when the stochastic forcing is isotropic and to antidiffusive fluxes when the forcing is anisotropic. In both cases this leads to the enhancement of the mean flow and to instability. On the other hand, advection of the mean vorticity by the eddies was found to have no effect to leading order when the forcing is isotropic and to lead to hyperdiffusive fluxes hindering jet formation when the forcing is anisotropic.

These processes were then examined in detail by studying the momentum fluxes induced by an ensemble of wavepackets in the presence of an infinitesimal sinusoidal mean flow. Assuming slow mean flow variations, we estimated the contribution of shearing of the wavepackets by the local shear and the contribution of wavepacket propagation under the inhomogeneous vorticity gradient in the ensemble mean momentum fluxes for both isotropic and anisotropic forcing. These calculations were performed in the physically relevant limit for the emergence of jets of small dissipation time scale compared to the shear time scale.

Shearing of the eddies in the manner described by the Orr dynamics in a  $\beta$  plane was found to have two effects. The first effect is that it changes the amplitude of the

fluxes in accordance with conservation of vorticity. This process leads to upgradient fluxes with an amplitude proportional to the shear unless the forcing is isotropic, in which case it produces no fluxes at all. This process underlies the negative viscosity characteristic of the fluxes in the case of anisotropic forcing. The second effect is that it changes the group velocity of the wavepacket compared to an unsheared perturbation propagating in a  $\beta$  plane. This process leads to momentum fluxes with an amplitude proportional to the third derivative of the mean flow that are upgradient for an isotropic forcing and downgradient for an anisotropic forcing. As a result, this process underlies the negative hyperviscosity characteristic of the fluxes in the case of isotropic forcing. In any case, the driving mechanism for the emergence of jets was found to be shearing of the eddies by the local shear in a  $\beta$  plane.

On the other hand, refraction of the eddies in the manner described by ray tracing of Rossby waves propagating under the inhomogeneous local mean vorticity gradient was found to change the amplitude of the fluxes according to wave action conservation. This process produces downgradient fluxes with an amplitude proportional to the third derivative of the mean flow, unless the forcing is isotropic, in which case it has no effect. As a result, this process underlies the hyperdiffusive action of the fluxes in the case of anisotropic forcing. Nevertheless, this process can be jet forming in the presence of topography with zonal mean flows emerging in regions where topography enhances  $\beta$ .

*Acknowledgments.* This research was supported by the EU FP-7 under the PIRG03-GA-2008-230958 Marie Curie Grant. The authors acknowledge the hospitality of the Aspen Center for Physics supported by the NSF (under Grant 1066293), where part of this work was written. The authors would also like to thank Kaushik Srinivasan and Bill Young for fruitful discussions and an early version of their manuscript and Brian Farrell and Freddy Bouchet for stimulating discussions on the results of this work.

## APPENDIX A

### Discrete Formulation of the SSST Equations

We here show the correspondence between the continuous and matrix formulations of the SSST equations. In the matrix formulation of SSST the Fourier transform of the vorticity field is defined as

$$q'(x, y, t) = \sum_{k=1}^{\infty} \text{Re}[\tilde{q}(k, y, t)e^{ikx}], \quad (\text{A1})$$

and the Fourier amplitudes at  $y_j$  evolve according to

$$\partial_t \tilde{q}(k, y_j, t) = \tilde{A}_{jk} \tilde{q}(k, y_j, t) + \tilde{f}(k, y_j, t), \quad (\text{A2})$$

with  $\tilde{A}_{jk} = -ikU_j - ik(\beta - U_{y_j y_j})\hat{\Delta}_j^{-1} - r$ ,  $\hat{\Delta}_j^{-1}$  the inverse of  $\hat{\Delta} = \partial_{y_j y_j}^2 - k^2$  and  $\tilde{f}$  the Fourier transform of  $f$  ( $\tilde{A}_{jk}$  denotes the  $k$  wavenumber operator  $A$  acting at points  $y_j$ ). A real vorticity field requires that  $\tilde{q}(-k, y, t) = \tilde{q}^*(k, y, t)$  and the covariance function can be written as

$$C(x_1, x_2, y_1, y_2, t) = \frac{1}{4} \sum_{k=-\infty}^{\infty} \sum_{k'=-\infty}^{\infty} \langle \tilde{q}(k, y_1, t) \tilde{q}(k', y_2, t) \rangle e^{ikx_1 + ik'x_2}, \quad (\text{A3})$$

with  $k = 0$  and  $k' = 0$  excluded in the summation. Since  $C$  is a function of  $x_1 - x_2$ , only terms with  $k' = -k$  contribute in (A3) and

$$C(x_1 - x_2, y_1, y_2, t) = \frac{1}{4} \sum_{k=-\infty}^{\infty} \tilde{C}_k e^{ik(x_1 - x_2)}, \quad (\text{A4})$$

with the definition  $\tilde{C}_k = \langle \tilde{q}(k, y_1, t) \tilde{q}^*(k, y_2, t) \rangle$  and with  $k = 0$  excluded. A similar decomposition is obtained for the forcing covariance, with the definition  $\tilde{Q}_k = \langle \tilde{f}(k, y_1) \tilde{f}^*(k, y_2) \rangle$ . By multiplying (A2) for  $\partial_t \tilde{q}(k, y_1, t)$  by  $\tilde{q}^*(k, y_2, t)$  and (A2) for  $\partial_t \tilde{q}^*(k, y_2, t)$  by  $\tilde{q}(k, y_1, t)$ , adding and taking the ensemble average, we obtain

$$\partial_t \tilde{C}_k = (\tilde{A}_{1k} + \tilde{A}_{2k}^*) \tilde{C}_k + \tilde{Q}_k. \quad (\text{A5})$$

Combining (9) and (A4), we obtain

$$\begin{aligned} \langle u'v' \rangle &= \frac{1}{4} \sum_{k=-\infty}^{\infty} \left( ik \partial_{y_2} \hat{\Delta}_1^{-1} \hat{\Delta}_2^{-1} \tilde{C}_k \right)_{y_1=y_2} \\ &= -\frac{1}{2} \sum_{k=1}^{\infty} \text{Im} \left( k \partial_{y_2} \hat{\Delta}_1^{-1} \hat{\Delta}_2^{-1} \tilde{C}_k \right)_{y_1=y_2}. \end{aligned} \quad (\text{A6})$$

By discretizing (A2) on a meridional grid, the Fourier components  $\tilde{q}(k, y_1, t)$  and  $\tilde{q}^*(k, y_2, t)$  become the column  $\mathbf{q}_k$  and row  $\mathbf{q}_k^\dagger$  vectors, respectively, with elements the values of the variables at the grid points and  $\dagger$  denotes the Hermitian transpose. The Fourier amplitudes of the forcing and vorticity covariance functions are approximated by the finite-dimensional covariance matrices  $\mathbf{Q}_k = \langle \mathbf{f}_k \mathbf{f}_k^\dagger \rangle$  and  $\mathbf{C}_k = \langle \mathbf{q}_k \mathbf{q}_k^\dagger \rangle$ , respectively, and the operators  $\tilde{A}_{1k}$  and  $\tilde{A}_{2k}^*$  are approximated by the matrices  $\mathbf{A}_k$  and  $\mathbf{A}_k^\dagger$ , respectively [as  $\tilde{A}_{2k}^* \tilde{q}^*(k, y_2, t)$  now reads  $\mathbf{q}_k^\dagger \mathbf{A}_k^\dagger$ ]. Equations (A5) and (10) then become

$$\frac{d\mathbf{C}_k}{dt} = \mathbf{A}_k \mathbf{C}_k + \mathbf{C}_k \mathbf{A}_k^\dagger + \mathbf{Q}_k, \quad (\text{A7})$$

$$\frac{d\mathbf{U}}{dt} = \sum_{k=1}^{\infty} \frac{k}{2} \text{vecd} \left[ \text{Im}(\mathbf{D}\mathbf{\Delta}_k^{-1}\mathbf{C}_k\mathbf{\Delta}_k^{-1\dagger}\mathbf{D}^\dagger) \right] - r\mathbf{U}. \quad (\text{A8})$$

In (A8),  $\mathbf{D}$  and  $\mathbf{\Delta}_k^{-1}$  are the finite-dimensional approximations of  $\partial_y$  and  $\hat{\Delta}^{-1}$ , respectively, and  $\text{vecd}$  denotes a vector containing the diagonal of the resulting matrix and is used to evaluate the fluxes at  $y_1 = y_2$ . This matrix system is equivalent to (12) and (13).

### APPENDIX B

#### Calculation of Momentum Fluxes for a Sinusoidal Flow

The purpose of this appendix is to calculate the perturbation momentum fluxes  $\overline{\delta u'v'}$  in the adiabatic limit for a harmonic mean flow perturbation  $\delta U_i = \sin(ny_i)$ . The perturbation streamfunction covariance in the adiabatic limit is determined from

$$\delta\Psi = \underbrace{P^{-1}(\delta U_1 - \delta U_2)\partial_{\tilde{x}} C^E}_{\delta\Psi^{\text{ad}}} - \underbrace{(\delta U_1'' - \delta U_2'')\tilde{\Delta}\partial_{\tilde{x}} \Psi^E}_{\delta\Psi^{\text{cu}}}, \quad (\text{B1})$$

$$\hat{\Psi}_n = \underbrace{\frac{ikK_+^4 \hat{\Psi}_+^E - ikK_-^4 \hat{\Psi}_-^E}{2in\beta kl + 2rK_+^2 K_-^2}}_{\hat{\Psi}_n^{\text{ad}}} - \underbrace{\frac{ikK_+^2 n^2 \hat{\Psi}_+^E - ikK_-^2 n^2 \hat{\Psi}_-^E}{2in\beta kl + 2rK_+^2 K_-^2}}_{\hat{\Psi}_n^{\text{cu}}}, \quad (\text{B4})$$

where  $\hat{\Psi}_n^{\text{ad}}$  and  $\hat{\Psi}_n^{\text{cu}}$  are the corresponding Fourier amplitudes of  $\delta\Psi^{\text{ad}}$  and  $\delta\Psi^{\text{cu}}$ ,  $K_\pm^2 = k^2 + (l \pm n/2)^2$ ,  $\hat{\Psi}_\pm^E = \hat{Q}(k, l \pm n/2)/(2rK_\pm^4)$ , and  $\hat{Q}(k, l)$  is the Fourier amplitude of  $Q$ . Introducing in (B4) the expression for  $\hat{\Psi}_n^E$  and taking the imaginary part, we obtain the perturbation momentum fluxes

$$\overline{\delta u'v'} = \delta\Psi_{\tilde{x}\tilde{y}}|_{\tilde{x}=\tilde{y}=0} = \text{Im}(ie^{in\tilde{y}}\Lambda_- - ie^{in\tilde{y}}\Lambda_+), \quad (\text{B5})$$

where

$$\Lambda_\pm = \frac{1}{4r\pi} \int_{-\infty}^{\infty} \int_{-\infty}^{\infty} \frac{k^2 l K_\pm^2 \hat{Q}(k, l \pm n/2)}{2in\beta kl K_\pm^2 + 2rK_+^2 K_-^2 K_\pm^2} dk dl - \frac{1}{4r\pi} \int_{-\infty}^{\infty} \int_{-\infty}^{\infty} \frac{k^2 l n^2 \hat{Q}(k, l \pm n/2)}{2in\beta kl K_\pm^2 + 2rK_+^2 K_-^2 K_\pm^2} dk dl. \quad (\text{B6})$$

where

$$P = 2\beta\partial_{\tilde{x}\tilde{y}\tilde{y}}^3 - 2r \left[ \tilde{\Delta}^2 + \frac{1}{2}(\partial_{\tilde{x}}^2 - \partial_{\tilde{y}}^2)\partial_{\tilde{y}}^2 + \frac{1}{16}\partial_{\tilde{y}}^4 \right], \quad (\text{B2})$$

$C^E = Q/2r$ , and  $C^E = \tilde{\Delta}^2\Psi^E$ . Because of the linearity of (B1), the perturbation streamfunction covariance can be written as  $\delta\Psi = \delta\Psi^{\text{ad}} + \delta\Psi^{\text{cu}}$ . The first term  $\delta\Psi^{\text{ad}}$  is the contribution to the perturbation covariance from the advection of the equilibrium vorticity covariance by the perturbation mean flow. The second term,  $\delta\Psi^{\text{cu}}$ , is the contribution from the advection of the vorticity of the perturbed flow by the eddies at equilibrium. Since this is a linear equation for the perturbation velocity, we choose the mean flow perturbation  $\delta U_i = e^{iny_i}$ , for which  $\delta U_1 - \delta U_2 = 2i \sin(n\tilde{y}/2)e^{in\tilde{y}}$ , and consider only the imaginary part. From now on we follow Srinivasan and Young (2012). We choose the streamfunction covariance to have the similar dependence  $\delta\Psi = \Psi_n(\tilde{x}, \tilde{y})e^{in\tilde{y}}$  and apply the Fourier transform

$$\Psi_n = \frac{1}{2\pi} \int_{-\infty}^{\infty} \int_{-\infty}^{\infty} \hat{\Psi}_n(k, l)e^{ik\tilde{x}+il\tilde{y}} dk dl \quad (\text{B3})$$

to obtain

The first and second terms are associated with the contribution of  $\delta\Psi^{\text{ad}}$  and  $\delta\Psi^{\text{cu}}$  to the momentum fluxes. Because the covariances satisfy the exchange symmetry  $Q(x_1, x_2, y_1, y_2) = Q(x_2, x_1, y_2, y_1)$ , which is the equivalent expression of the hermiticity of the corresponding covariances in the matrix formulation, we obtain  $Q(\tilde{x}, \tilde{y}) = Q(-\tilde{x}, -\tilde{y})$ , yielding

$$\hat{Q}(-k, -l) = \hat{Q}(k, l), \quad (\text{B7})$$

which implies, because  $Q$  is a real function and  $\hat{Q}^*(k, l) = \hat{Q}(-k, -l)$ , that  $\hat{Q}$  is also real. Changing the sign of  $k$  and  $l$  in (B6) and using (B7), we obtain that  $\Lambda_+ = -\Lambda_-$ . We assume that the smallest scale in which the forcing has significant power is  $L_f = 1/\sqrt{k_f^2 + l_f^2}$  and we nondimensionalize the wavenumbers in (B6) with this scale, so that  $(k, l, n) = (\tilde{k}, \tilde{l}, \tilde{n})/L_f$ . Using  $\Lambda_+ = -\Lambda_-$  and shifting the origin of the  $l$  axis  $l \rightarrow l - n/2$  in the integral reduces (B5) to

$$\begin{aligned}
& (\delta\overline{u'v'}^{\text{ad}}, \delta\overline{u'v'}^{\text{cu}}) \\
&= \text{Im} \left[ \frac{ie^{i\tilde{n}\tilde{y}/L_f}}{4rL_f\pi} \int_{-\infty}^{\infty} \int_{-\infty}^{\infty} (K^2, -\tilde{n}^2) F(\tilde{k}, \tilde{l}) d\tilde{k} d\tilde{l} \right], \quad (\text{B8})
\end{aligned}$$

where

$$F(\tilde{k}, \tilde{l}) = \frac{\tilde{k}^2(\tilde{l} + \tilde{n}/2)\hat{Q}(\tilde{k}, \tilde{l})}{i\tilde{n}\beta L_f \tilde{k}(\tilde{l} + \tilde{n}/2)K^2 + r(K^2 + 2\tilde{l}\tilde{n} + \tilde{n}^2)K^4}, \quad (\text{B9})$$

$K = \sqrt{\tilde{k}^2 + \tilde{l}^2}$  is the total wavenumber, and  $\delta\overline{u'v'}^{\text{ad}}$  and  $\delta\overline{u'v'}^{\text{cu}}$  are the contributions of  $\delta\Psi^{\text{ad}}$  and  $\delta\Psi^{\text{cu}}$  to the momentum fluxes, so that  $\delta\overline{u'v'} = \delta\overline{u'v'}^{\text{ad}} + \delta\overline{u'v'}^{\text{cu}}$ . Note that if the forcing obeys the mirror symmetry  $\hat{Q}(-\tilde{k}, \tilde{l}) = \hat{Q}(\tilde{k}, \tilde{l})$ —as is the case for isotropic forcing or if the correlation function  $Q$  is a separable function of  $\tilde{x}$  and  $\tilde{y}$ , as is the case of the anisotropic forcing in (24)—the integral of (B8) is a real number and the fluxes are proportional to  $\cos(n\tilde{y})$ ; that is, they are proportional to an odd derivative of the mean flow perturbation. This implies that the momentum flux divergence in these cases is proportional to an even derivative of the mean flow perturbation.

We obtain approximate expressions of the integrals when the scale of the mean flow is much larger than the scale of the forcing,  $\tilde{n} \ll 1$ , and the propagation time scale  $1/\beta L_f$  is at most of the same order as the dissipation time scale  $1/r$  ( $\beta L_f/r < 1$ ), so that  $\beta L_f \tilde{n}/r \ll 1$ . In this limit the leading term in the denominator of  $F$  is  $rK^6$ , while all the other terms are order  $\tilde{n}$  or order  $\tilde{n}^2$  smaller than this.<sup>B1</sup> Expanding  $F$  in powers of  $\tilde{n}$  and keeping the terms that are even functions of  $\tilde{k}$  and  $\tilde{l}$  and will therefore contribute to the integral for a forcing that obeys the mirror symmetry, we obtain

$$\begin{aligned}
\delta\overline{u'v'}^{\text{ad}} &= \frac{n \cos(n\tilde{y})}{8\pi r^2} \left( A_S - \tilde{n}^2 \frac{\beta^2 L_f^2}{r^2} A_\beta - \tilde{n}^2 A_C \right), \\
\delta\overline{u'v'}^{\text{cu}} &= -\frac{n \cos(n\tilde{y})}{8\pi r^2} \tilde{n}^2 A_P, \quad (\text{B10})
\end{aligned}$$

where

$$\begin{aligned}
A_S &= \int_{-\infty}^{\infty} \int_{-\infty}^{\infty} \frac{\tilde{k}^2(\tilde{k}^2 - 3\tilde{l}^2)}{(\tilde{k}^2 + \tilde{l}^2)^3} \hat{Q} d\tilde{k} d\tilde{l}, \\
A_\beta &= \int_{-\infty}^{\infty} \int_{-\infty}^{\infty} \frac{3\tilde{k}^4 \tilde{l}^2 (\tilde{k}^2 - 3\tilde{l}^2)}{(\tilde{k}^2 + \tilde{l}^2)^7} \hat{Q} d\tilde{k} d\tilde{l}, \quad (\text{B11})
\end{aligned}$$

<sup>B1</sup> The limit  $\beta L_f/r < 1$  ensures that the first terms in the denominator are at least order  $\tilde{n}$  smaller than the leading-order term  $rK^6$ .

$$\begin{aligned}
A_C &= \int_{-\infty}^{\infty} \int_{-\infty}^{\infty} \frac{\tilde{k}^2(\tilde{k}^4 - 10\tilde{k}^2\tilde{l}^2 + 5\tilde{l}^4)}{(\tilde{k}^2 + \tilde{l}^2)^5} \hat{Q} d\tilde{k} d\tilde{l}, \\
A_P &= \int_{-\infty}^{\infty} \int_{-\infty}^{\infty} \frac{\tilde{k}^2(\tilde{k}^2 - 3\tilde{l}^2)}{(\tilde{k}^2 + \tilde{l}^2)^4} \hat{Q} d\tilde{k} d\tilde{l}. \quad (\text{B12})
\end{aligned}$$

Note that, when the forcing does not obey the mirror symmetry, terms proportional to  $\tilde{n}$  might appear in the parenthesis in (B10) (K. Srinivasan 2013, personal communication). We will now show that the approximate expression in (B10) can also be obtained by considering a slowly varying mean flow  $U_i = U_i(\nu y_i)$ , where  $\nu \ll 1$ , for which

$$U_1 - U_2 = \nu \tilde{y} U'(\nu \tilde{y}) + (\nu \tilde{y})^3 U'''(\nu \tilde{y})/24 + \dots, \quad (\text{B13})$$

$$U_1'' - U_2'' = \nu^3 \tilde{y} U'''(\nu \tilde{y}) + \nu^5 \tilde{y}^3 U^{(5)}(\nu \tilde{y})/24 + \dots. \quad (\text{B14})$$

That is, the eddies are advected to first order by the slowly varying local shear  $y$ . They also advect the local mean vorticity that has to leading order a linear gradient with respect to latitude and is also slowly varying. A two-scale perturbation expansion of (B1) with slow variable  $Y = \nu y$  and  $\delta\Psi = \nu\Psi^1 + \nu^2\Psi^2 + \nu^3\Psi^3 + \dots$  gives that the Fourier amplitudes of  $\Psi^i$  to the third order are<sup>B2</sup>

$$\begin{aligned}
\hat{\Psi}^1 &= \frac{U'(Y)}{4r^2} \frac{k}{(k^2 + l^2)^2} \frac{\partial \hat{Q}}{\partial l}, \\
\hat{\Psi}^2 &= -\frac{\beta U''(Y)}{4r^3} \frac{k^2 l}{(k^2 + l^2)^4} \frac{\partial \hat{Q}}{\partial l}, \quad (\text{B15}) \\
\hat{\Psi}^3 &= \frac{U'''(Y)}{8r^2} \frac{k(k^2 - l^2)}{(k^2 + l^2)^4} \frac{\partial \hat{Q}}{\partial l} - \frac{U'''(Y)}{96r^2} \frac{k}{(k^2 + l^2)^2} \frac{\partial^3 \hat{Q}}{\partial l^3} \\
&\quad + \frac{\beta^2 U'''(Y)}{4r^4} \frac{k^3 l^2}{(k^2 + l^2)^6} \frac{\partial \hat{Q}}{\partial l} \\
&\quad + \frac{U'''(Y)}{4r^2} \frac{k}{(k^2 + l^2)^2} \frac{\partial}{\partial l} \left( \frac{\hat{Q}}{k^2 + l^2} \right). \quad (\text{B16})
\end{aligned}$$

The resulting momentum fluxes are

$$\begin{aligned}
\delta\overline{u'v'} &= \partial_{xy}^2 \delta\Psi|_{\tilde{x}=\tilde{y}=0} = \nu A_S \frac{U'(Y)}{8\pi r^2} + \nu^3 A_\beta \frac{\beta^2 U'''(Y)}{8\pi K_f^4 r^4} \\
&\quad + \nu^3 A_C \frac{U'''(Y)}{8\pi r^2} + \nu^3 A_P \frac{U'''(Y)}{8\pi r^2}, \quad (\text{B17})
\end{aligned}$$

which gives (B10) when  $U(\nu y) = \sin(ny)$ . This proves that the limit  $\tilde{n} \ll 1$  and  $\beta L_f \tilde{n}/r \ll 1$  is equivalent to considering local dynamics for the forced eddies.

<sup>B2</sup> We also assume that the terms in the  $P$  operator in (B2),  $\beta$  and  $r O(1)$  so that the only small terms are the ones associated with  $\nu$ . This is equivalent to the approximation  $\beta L_f/r < 1$ .

We now calculate the coefficients  $A_S, A_\beta, A_C,$  and  $A_P$  for the two cases of stochastic forcing discussed in section 3. The first is the isotropic ring forcing in (21) with  $\hat{Q} = \delta(\sqrt{k^2 + l^2} - K_f)$  and  $L_f = 1/K_f$  and the second is the anisotropic forcing in (24) with  $\hat{Q} = (a_{k_f} \delta \sqrt{\pi/2})[\delta(k - k_f) + \delta(k + k_f)]e^{-l^2 \delta^2/2}$  and  $L_f = \min(1/k_f, \delta)$ . The amplitude  $a_{k_f}$  is chosen so that the energy density of the forcing per unit time is a fraction  $\sigma$  of the energy in a constant flow of unit velocity. To calculate  $a_{k_f}$ , we first obtain the energy density of the forcing with a covariance function  $\Psi_f$ :

$$E = \frac{1}{2} (\langle u'_1 u'_2 \rangle + \langle v'_1 v'_2 \rangle)_{x_1 = x_2} = -\frac{1}{2} \tilde{\Delta} \Psi_f \Big|_{\tilde{x} = \tilde{y} = 0}$$

$$= \frac{1}{4\pi} \int_{-\infty}^{\infty} \int_{-\infty}^{\infty} \frac{\hat{Q}}{k^2 + l^2} dk dl. \tag{B18}$$

The zonally averaged energy in (B18) equals  $\sigma/2$  according to the normalization yielding

$$a_{k_f} = \frac{2\sigma k_f e^{-k_f^2 \delta^2/2}}{\delta \sqrt{2\pi} \operatorname{erfc}(k_f \delta / \sqrt{2})}. \tag{B19}$$

For the isotropic forcing in (21), it can be shown that  $A_S = A_P = A_C = 0$  and  $A_\beta = -3\pi/16K_f$ . We thus obtain (22). For the anisotropic forcing in (24), we obtain

$$A_S = \sigma k_f^2 \delta^2 \left[ \pi(1 + k_f^2 \delta^2) - \frac{k_f \delta e^{-k_f^2 \delta^2/2} \sqrt{2\pi}}{\operatorname{erfc}(k_f \delta / \sqrt{2})} \right], \tag{B20}$$

$$A_\beta = -\frac{3\sigma \delta^2}{5760 k_f^2 L_f^4} (-45 + 45k_f^2 \delta^2 - 30k_f^4 \delta^4 + 30k_f^6 \delta^6 + 15k_f^8 \delta^8 + k_f^{10} \delta^{10}) \pi$$

$$+ \frac{3\sigma \delta^3}{5760 k_f L_f^4} \frac{\sqrt{2\pi} (45 - 30k_f^2 \delta^2 + 18k_f^4 \delta^4 + 14k_f^6 \delta^6 + k_f^8 \delta^8)}{e^{k_f^2 \delta^2/2} \operatorname{erfc}(k_f \delta / \sqrt{2})}, \tag{B21}$$

$$A_C = \frac{\sigma k_f^2 \delta^4}{12L_f^2} \left[ -(3 + 6k_f^2 \delta^2 + k_f^4 \delta^4) \pi + \frac{k_f \delta \sqrt{2\pi} (5 + k_f^2 \delta^2)}{e^{k_f^2 \delta^2/2} \operatorname{erfc}(k_f \delta / \sqrt{2})} \right], \text{ and} \tag{B22}$$

$$A_P = \frac{\sigma}{12k_f^2 L_f^2} \left[ -(-3 + 3k_f^4 \delta^4 + 2k_f^6 \delta^6) \pi + \frac{k_f \delta \sqrt{2\pi} (3 + k_f^2 \delta^2 + 2k_f^4 \delta^4)}{e^{k_f^2 \delta^2/2} \operatorname{erfc}(k_f \delta / \sqrt{2})} \right]. \tag{B23}$$

In the limit of  $k_f \delta \gg 1$ , (B20)–(B23) are approximately equal to

$$[A_S, A_\beta, A_C, A_P] \simeq 2\sigma \pi \left[ 1, \frac{3}{k_f^6 \delta^2 L_f^4}, \frac{1}{k_f^2 L_f^2}, \frac{1}{k_f^2 L_f^2} \right],$$

yielding (25) and (26). In the limit of  $k_f \delta \ll 1$ , (B20)–(B23) are approximately equal to

$$[A_S, A_\beta, A_C, A_P] \simeq \sigma \pi \left[ k_f^2 \delta^2, \frac{3\delta^2}{128 k_f^2 L_f^4}, \frac{k_f^2 \delta^4}{4L_f^2}, \frac{1}{4k_f^2 L_f^2} \right].$$

For  $\delta \rightarrow 0$ , the only nonzero coefficient is  $A_P = 1/4k_f^2 L_f^2$  producing downgradient hyperdiffusive fluxes.

## APPENDIX C

### Eddy Fluxes Produced by an Ensemble of Wave Packets

In this appendix we show that an alternative way to calculate the ensemble mean momentum fluxes in the slowly varying limit is to calculate the momentum fluxes of wavepackets that are initially localized at different latitudes, then integrate the fluxes over the life cycle of the wavepackets and add their contribution as if they evolved independently. Following the calculation in section 3, we consider a stationary mean flow perturbation  $\delta U$  around the statistical equilibrium in (14) and calculate the perturbation covariance  $\delta C$  that is induced by  $\delta U$ . The solution of (8) for stationary mean flows, and time invariant  $A_i$ , is

$$C = \int_0^t e^{(A_1 + A_2)s} Q ds. \tag{C1}$$

The steady-state covariance is obtained from the  $t \rightarrow \infty$  limit of (C1). In the adiabatic limit, in which the

covariances at all times assume their equilibrium value ( $d\delta C/dt \simeq 0$ ),  $\delta C$  is the difference between covariance  $C^{\delta U}$  that results at steady state when the mean flow is  $\delta U$  and the equilibrium covariance  $C^E$ . That is, we can write

$$\delta C = \lim_{t \rightarrow \infty} (C^{\delta U} - C^E) = \int_0^\infty e^{(\delta A_1 + \delta A_2)t} Q dt - \int_0^\infty e^{(A_1^E + A_2^E)t} Q dt, \tag{C2}$$

where

$$\begin{aligned} \delta A_i &= -\delta U_i \partial_{x_i} - (\beta - \delta U_{y_i}) \Delta_i^{-1} \partial_{x_i} - r, \\ A_i^E &= -\beta \Delta_i^{-1} \partial_{x_i} - r, \end{aligned} \tag{C3}$$

and  $\delta U_i = \sin(ny_i)$  is the mean flow perturbation. Substituting (C2) into (9), we obtain the alternative expression for the momentum fluxes

$$\delta \langle u'v' \rangle = - \int_0^\infty \left( \partial_{x_1} \Delta_1^{-1} e^{\delta A_1 t} \partial_{y_2} \Delta_2^{-1} e^{\delta A_2 t} Q \right)_{\mathbf{x}_1 = \mathbf{x}_2} dt. \tag{C4}$$

To obtain (C4), we have used the property that all operators acting at different points commute and that the equilibrium covariance does not produce any ensemble mean fluxes. We then apply a Fourier transform to the forcing  $f$  and obtain the forcing covariance as

---


$$Q = \langle f_1 f_2 \rangle = \frac{1}{4\pi^2} \int_{-\infty}^\infty \int_{-\infty}^\infty \int_{-\infty}^\infty \int_{-\infty}^\infty \langle \hat{f}(k, l) \hat{f}(k', l') \rangle e^{ikx_1 + ik'x_2 + ily_1 + il'y_2} dk dk' dl dl'. \tag{C5}$$


---

Because  $Q$  is homogeneous and depends only on  $x_1 - x_2$  and  $y_1 - y_2$ , the ensemble mean Fourier amplitudes satisfy

$$\langle \hat{f}(k, l) \hat{f}(k', l') \rangle = 2\pi \delta(k + k') \delta(l + l') \hat{Q}(k, l). \tag{C6}$$

Positive definiteness of  $Q$  implies that  $\hat{Q} > 0$  and (C6) is equivalently written as

$$\begin{aligned} \langle \hat{f}(k, l) \hat{f}(k', l') \rangle &= \int_{-\infty}^\infty \delta(k + k') e^{-i(l+l')\xi} \sqrt{\hat{Q}(k, l)} \sqrt{\hat{Q}(k', l')} d\xi. \end{aligned} \tag{C7}$$

Using (C7), (C5) becomes

---


$$\begin{aligned} Q = \langle f_1 f_2 \rangle &= \frac{1}{4\pi^2} \int_{-\infty}^\infty \int_{-\infty}^\infty \int_{-\infty}^\infty \sqrt{\hat{Q}(k, l)} \sqrt{\hat{Q}(-k, l')} e^{ik(x_1 - x_2)} e^{il(y_1 - \xi)} e^{il'(y_2 - \xi)} d\xi dk dl dl' \\ &= \frac{1}{2\pi} \int_{-\infty}^\infty \int_{-\infty}^\infty G(k, y_1 - \xi) G^*(k, y_2 - \xi) e^{ik(x_1 - x_2)} d\xi dk, \end{aligned} \tag{C8}$$


---

where we have used  $\hat{Q}(-k, l) = \hat{Q}(k, -l)$  because of the exchange symmetry in (B7) and

$$G(k, y) = \frac{1}{\sqrt{2\pi}} \int_{-\infty}^\infty \sqrt{\hat{Q}(k, l)} e^{ily} dl. \tag{C9}$$

Consequently, (C4) becomes

$$\delta \langle u'v' \rangle = \frac{1}{2\pi} \int_0^\infty \overline{u'v'} dt d\xi dk, \tag{C10}$$

where

$$\begin{aligned} \overline{u'v'} &= -[ik \Delta_{1k}^{-1} e^{\delta A_1^k} G(k, y_1 \\ &\quad - \xi) \partial_{y_2} \Delta_{2k}^{-1} e^{(\delta A_2^k)^*} G^*(k, y_2 - \xi)]_{y_1 = y_2}, \end{aligned} \tag{C11}$$

$\Delta_{ik}^{-1}$  is the inverse of  $\Delta_{ik} = \partial_{y_i y_i}^2 - k^2$ , and

$$\delta A_{jk} = -ik \delta U_j - ik(\beta - \delta U_{y_j}) \Delta_{jk}^{-1} - r. \tag{C12}$$

The integrand (C11) is twice the momentum flux at time  $t$  produced by the initial monochromatic perturbation  $G(k, y) e^{ikx}$ , which is localized at latitude  $\xi$ . We have therefore shown that the perturbation momentum fluxes can be calculated as follows: take an ensemble of perturbations  $G(k, y) e^{ikx}$ , each localized around different latitudes, calculate the momentum fluxes over their life cycles, and then add their relative contribution, as if the waves evolved independently, to obtain the ensemble mean perturbation fluxes. We will now show that for both the ring forcing in (21) and the anisotropic forcing in (24), the perturbations  $G$  can be interpreted as wavepackets.

Consider the ring forcing in (32) that has a finite width  $2\Delta K$  in wavenumber space. The ring sector  $|K - K_f| \leq \Delta K$  is equivalently determined by the inequalities

$$|l \pm \sqrt{K_f^2 - k^2}| \leq \delta(k), \quad \text{for } |k| \leq K_f, \quad (C13)$$

where  $\delta(k) = K_f \Delta K / \sqrt{K_f^2 - k^2}$  is the width of the ring sector at each wavenumber  $k$ . To calculate the momentum fluxes in closed form, we consider the modification of (32):

$$\hat{Q}(k, l) = \frac{1}{\Delta K \sqrt{\pi}} \left[ e^{-(l - \sqrt{K_f^2 - k^2})^2 / \delta(k)^2} + e^{-(l + \sqrt{K_f^2 - k^2})^2 / \delta(k)^2} \right] \Theta(K_f - |k|), \quad (C14)$$

with the width  $\delta(k)$ . For the forcing in (C14) in the limit  $\Delta K \ll 1$ , we integrate (C9) to obtain to a good approximation that  $G$  is a wavepacket with central wavenumber  $l_0 = \sqrt{K_f^2 - k^2}$ :

$$G(k, y) = \sqrt{\frac{\Delta K}{\sqrt{\pi}}} \frac{2K_f}{\sqrt{K_f^2 - k^2}} \cos(l_0 y) e^{-\delta(k)^2 y^2 / 2} \Theta(K_f - |k|). \quad (C15)$$

The initial momentum flux of this wavepacket for the isotropic forcing is

---


$$\begin{aligned} \frac{1}{2\pi} \int_{-\infty}^{\infty} \int_{-\infty}^{\infty} \overline{u'v'}(t=0) d\xi dk &= - \int_{-K_f}^{K_f} \int_{-\infty}^{\infty} \frac{kl_0 \Delta K e^{-\delta^2(y-\xi)^2}}{2\pi K_f^2 \sqrt{\pi}(K_f^2 - k^2)} [-1 + 1 + e^{2il_0(y+\xi)} - e^{-2il_0(y+\xi)}] d\xi dk \\ &= - \int_{-K_f}^{K_f} \frac{kl_0}{2\pi K_f^2 \sqrt{K_f^2 - k^2}} (-1 + 1 + e^{-l_0^2/\delta^2} e^{-2il_0 y} - e^{-l_0^2/\delta^2} e^{2il_0 y}) dk. \end{aligned} \quad (C16)$$

The first two terms in the integrand are the contribution of  $l_0$  and  $-l_0$  in the momentum fluxes, while the last two terms are the interference terms between these two waves. By taking the limit  $\Delta K \rightarrow 0$ ,  $\delta \rightarrow 0$  the interference terms go to zero, resulting in zero net momentum fluxes imposed at  $t = 0$ . For the same reason, the interference terms make no contribution when the perturbations evolve in a shear flow. So we can take  $G$  to be given by (33), for which we consider only the single wave  $l_0$ . The relative contribution of  $-l_0$  in the ensemble mean momentum fluxes is taken into account by adding the corresponding term in (41) for  $-l_0$  in order to obtain (42). Consider now the anisotropic forcing in (24), for which  $\hat{Q} = (a_{k_f} \delta \sqrt{\pi}/2) [\delta(k - k_f) + \delta(k + k_f)] e^{-l^2 \delta^2 / 2}$ . Then  $G$  is given by

$$G(k, y) = \sqrt{\frac{a_{k_f}}{\delta}} (2\pi)^{1/4} [\delta(k - k_f) + \delta(k + k_f)] e^{-y^2 / \delta^2}. \quad (C17)$$

#### APPENDIX D

##### Wave Propagation in an Inhomogeneous Medium

Consider the evolution of an ensemble of wavepackets propagating in a motionless flow with a background vorticity gradient  $Q_y = \beta - \gamma(y - \xi)$ , with  $\gamma L_f^2 / r \ll \beta L_f / r \ll 1$ . We will calculate the momentum

fluxes produced by this wavepacket over its life cycle using ray tracing. The rate of change of the meridional position of the wavepacket  $y$  and the slowly varying wavenumber  $l_i(t)$  along a ray are given by the standard ray-tracing equations (Andrews et al. 1987)

$$\frac{d_g y}{dt} = \frac{\partial \omega}{\partial l_i}, \quad \frac{d_g l_i}{dt} = - \frac{\partial \omega}{\partial y}, \quad (D1)$$

where  $\omega = -[\beta - \gamma(y - \xi)]k / (k^2 + l_i^2)$  is the frequency of the propagating waves and  $d_g/dt$  denotes time differentiation along a group-velocity ray. We obtain from (D1) that the wavenumber  $l_i$  and the displacement of the wavepacket  $\eta(t) \equiv y$  satisfy

$$\begin{aligned} l_i^3 + 3k^2 l_i - l_0^3 - 3k^2 l_0 + 3\gamma k t &= 0, \\ \eta(t) &= \xi + \frac{\beta}{\gamma} \left[ 1 - e^{-(\gamma/\beta) \int_0^t c_g(s) ds} \right], \end{aligned} \quad (D2)$$

with  $l_0 = l_i(0)$ ,  $\xi$  the initial position of the wavepacket, and  $c_g = 2\beta k l_i / (k^2 + l_i^2)^2$  is the time dependent  $y$  component of the group velocity. The wavepacket therefore evolves as

$$q(x, y, t) = B_t e^{ikx + il_i(y - \xi)} h(y - \xi - \eta), \quad (D3)$$

where  $B_t(t)$  is the time-dependent amplitude with  $B_t(0) = B$ . To leading order, the spatial density of wave action along rays satisfies the equation

$$\frac{E(t)}{\omega(t)} = \frac{E(0)}{\omega(0)} e^{-2rt}, \quad (\text{D4})$$

where  $E(t)$  is the energy density of the wavepacket following a ray that is given by

$$E(t) = \frac{1}{4} \left( |\partial_x \psi|^2 + |\partial_y \psi|^2 \right) = \frac{|B_t|^2}{k^2 + l_t^2}. \quad (\text{D5})$$

Equation (D4) then implies that the amplitude decays exponentially  $B_t = B(0)e^{-rt}$ . As a result, the momentum fluxes produced by the wavepacket are given by (38). The dominant contribution to (30) comes from small times in the limit  $\gamma L_f^2/r \ll \beta L_f/r \ll 1$ , since the wave is dissipated before it propagates. For small times, (D2) gives

$$l_t \simeq l - \gamma \frac{kt}{k^2 + l_0^2} + O(\gamma^2 t^2), \quad \eta \simeq \xi + c_g(0)t + O(\gamma\beta), \quad (\text{D6})$$

and, consequently,

$$\frac{kl_t}{(k^2 + l_t^2)^2} \simeq \frac{kl_0}{(k^2 + l_0^2)^2} + \frac{k^2(3l_0^2 - k^2)}{(k^2 + l_0^2)^4} \gamma t + O(\gamma^2 t^2). \quad (\text{D7})$$

Inserting the approximate expressions (D6)–(D7) in (38), integrating over time, and keeping terms that are even in  $k$  and  $l_0$ , we obtain (49).

#### REFERENCES

- Andrews, D. G., J. R. Holton, and C. B. Leovy, 1987: *Middle Atmosphere Dynamics*. Academic Press, 489 pp.
- Bakas, N. A., and P. J. Ioannou, 2011: Structural stability theory of two-dimensional fluid flow under stochastic forcing. *J. Fluid Mech.*, **682**, 332–361, doi:10.1017/jfm.2011.228.
- Berloff, P., I. Kamenkovich, and J. Pedlosky, 2009a: A mechanism of formation of multiple zonal jets in the oceans. *J. Fluid Mech.*, **628**, 395–425.
- , —, and —, 2009b: A model of multiple zonal jets in the oceans: Dynamical and kinematical analysis. *J. Phys. Oceanogr.*, **39**, 2711–2734.
- Bouchet, F., and E. Simonnet, 2009: Random changes of flow topology in two-dimensional and geophysical turbulence. *Phys. Rev. Lett.*, **102**, 094504, doi:10.1103/PhysRevLett.102.094504.
- , and A. Venaille, 2012: Statistical mechanics of two-dimensional and geophysical flows. *Phys. Rep.*, **515**, 227–295, doi:10.1016/j.physrep.2012.02.001.
- Boyd, J. P., 1983: The continuous spectrum of linear Couette flow with the beta effect. *J. Atmos. Sci.*, **40**, 2304–2308.
- Cho, J. Y. K., and L. M. Polvani, 1996: The morphogenesis of bands and zonal winds in the atmospheres of the giant outer planets. *Science*, **273**, 335–337.
- Connaughton, C., B. Nadiga, S. Nazarenko, and B. Quinn, 2010: Modulational instability of Rossby and drift waves and generation of zonal jets. *J. Fluid Mech.*, **654**, 207–231.
- Cummins, P. F., and G. Holloway, 2010: Reynolds stress and eddy viscosity in direct numerical simulation of sheared two-dimensional turbulence. *J. Fluid Mech.*, **657**, 394–412.
- DelSole, T., 1996: Can quasigeostrophic turbulence be modeled stochastically? *J. Atmos. Sci.*, **53**, 1617–1633.
- , 1999: Stochastic models of shear-flow turbulence with enstrophy transfer to subgrid scales. *J. Atmos. Sci.*, **56**, 3692–3703.
- , 2001: A theory for the forcing and dissipation in stochastic turbulence models. *J. Atmos. Sci.*, **58**, 3762–3775.
- , 2004: Stochastic models of quasigeostrophic turbulence. *Surv. Geophys.*, **25**, 107–194.
- , and B. F. Farrell, 1996: The quasi-linear equilibration of a thermally maintained, stochastically excited jet in a quasigeostrophic model. *J. Atmos. Sci.*, **53**, 1781–1797.
- Dritchel, D. G., and M. E. McIntyre, 2008: Multiple jets as PV staircases: The Phillips effect and the resilience of eddy-transport barriers. *J. Atmos. Sci.*, **65**, 855–874.
- Dunkerton, T. J., and R. K. Scott, 2008: A barotropic model of the angular momentum-conserving potential vorticity staircase in spherical geometry. *J. Atmos. Sci.*, **65**, 1105–1136.
- Farrell, B. F., 1987: Developing disturbances in shear. *J. Atmos. Sci.*, **44**, 2191–2199.
- , and P. J. Ioannou, 1993a: Stochastic dynamics of baroclinic waves. *J. Atmos. Sci.*, **50**, 4044–4057.
- , and —, 1993b: Stochastic forcing of perturbation variance in unbounded shear and deformation flows. *J. Atmos. Sci.*, **50**, 200–211.
- , and —, 2003: Structural stability of turbulent jets. *J. Atmos. Sci.*, **60**, 2101–2118.
- , and —, 2007: Structure and spacing of jets in barotropic turbulence. *J. Atmos. Sci.*, **64**, 3652–3655.
- , and —, 2009: A theory of baroclinic turbulence. *J. Atmos. Sci.*, **66**, 2444–2454.
- Galperin, B. H., S. Sukoriansky, N. Dikovskaya, P. Read, Y. Yamazaki, and R. Wordsworth, 2006: Anisotropic turbulence and zonal jets in rotating flows with a  $\beta$ -effect. *Nonlinear Processes Geophys.*, **13**, 83–98.
- Gill, A. E., 1974: The stability of planetary waves on an infinite beta plane. *Geophys. Fluid Dyn.*, **6**, 29–47.
- Holloway, G., 2010: Eddy stress and shear in 2D flows. *J. Turbul.*, **11**, 1–14.
- Huang, H. P., and W. A. Robinson, 1998: Two-dimensional turbulence and persistent zonal jets in a global barotropic model. *J. Atmos. Sci.*, **55**, 611–632.
- Ingersoll, A. P., 1990: Atmospheric dynamics of the outer planets. *Science*, **248**, 308–315.
- Kramer, W., J. H. Clercx, and G. J. F. van Heijst, 2008: On the large scale structure and spectral dynamics of two-dimensional turbulence in a periodic channel. *Phys. Fluids*, **20**, 056602, doi:10.1063/1.2919132.
- Kuo, H.-L., 1951: Vorticity transfer as related to the development of the general circulation. *J. Meteor.*, **8**, 307–315.
- Lorenz, E. N., 1972: Barotropic instability of Rossby wave motion. *J. Atmos. Sci.*, **29**, 258–264.
- Manfroi, A. J., and W. R. Young, 1999: Slow evolution of zonal jets on the beta plane. *J. Atmos. Sci.*, **56**, 784–800.
- Marston, J. B., 2010: Statistics of the general circulation from cumulant expansions. *Chaos*, **20**, 041107, doi:10.1063/1.3490719.

- , 2012: Planetary atmospheres as non-equilibrium condensed matter. *Annu. Rev. Condens. Matter Phys.*, **3**, 285–310.
- , E. Conover, and T. Schneider, 2008: Statistics of an unstable barotropic jet from a cumulant expansion. *J. Atmos. Sci.*, **65**, 1955–1966.
- Nazarenko, S., and B. Quinn, 2009: Triple cascade behavior in quasigeostrophic and drift turbulence and generation of zonal jets. *Phys. Rev. Lett.*, **103**, 118501, doi:10.1103/PhysRevLett.103.118501.
- Nozawa, T., and Y. Yoden, 1997: Formation of zonal band structure in forced two-dimensional turbulence on a rotating sphere. *Phys. Fluids*, **9**, 2081–2093.
- O’Gorman, P. A., and T. Schneider, 2007: Recovery of atmospheric flow statistics in a general circulation model without nonlinear eddy-eddy interactions. *Geophys. Res. Lett.*, **34**, L22801, doi:10.1029/2007GL031779.
- Read, P. L., Y. H. Yamazaki, S. R. Lewis, P. D. Williams, K. Miki-Yamazaki, J. Sommeria, H. Didelle, and A. Fincham, 2004: Jupiter’s and Saturn’s convectively driven banded jets in the laboratory. *Geophys. Res. Lett.*, **31**, L22701, doi:10.1029/2004GL020106.
- , —, —, —, R. Wordsworth, and K. Miki-Yamazaki, 2007: Dynamics of convectively driven banded jets in the laboratory. *J. Atmos. Sci.*, **64**, 4031–4052.
- Rhines, P. B., 1975: Waves and turbulence on a beta plane. *J. Fluid Mech.*, **69**, 417–433.
- Scott, R. K., and L. M. Polvani, 2008: Equatorial superrotation in shallow atmospheres. *Geophys. Res. Lett.*, **35**, L24202, doi:10.1029/2008GL036060.
- , and D. G. Dritchel, 2012: The structure of zonal jets in geostrophic turbulence. *J. Fluid Mech.*, **711**, 576–598, doi:10.1017/jfm.2012.410.
- Shepherd, T. G., 1985: Time development of small disturbances to plane Couette flow. *J. Atmos. Sci.*, **42**, 1868–1871.
- , 1987a: Rossby waves and two-dimensional turbulence in a large-scale zonal jet. *J. Fluid Mech.*, **183**, 467–509.
- , 1987b: A spectral view of nonlinear fluxes and stationary-transient interaction in the atmosphere. *J. Atmos. Sci.*, **44**, 1166–1178.
- Srinivasan, K., and W. R. Young, 2012: Zonostrophic instability. *J. Atmos. Sci.*, **69**, 1633–1656.
- Starr, V., 1968: *Physics of Negative Viscosity Phenomena*. McGraw-Hill, 256 pp.
- Thompson, A. F., 2010: Jet formation and evolution in baroclinic turbulence with simple topography. *J. Phys. Oceanogr.*, **40**, 257–278.
- Tung, K. K., 1983: Initial value problems for Rossby waves in a shear flow with critical level. *J. Fluid Mech.*, **133**, 443–469.
- Vallis, G. K., and M. E. Maltrud, 1993: Generation of mean flows and jets on a beta plane and over topography. *J. Phys. Oceanogr.*, **23**, 1346–1362.
- Vasavada, A. R., and A. P. Showman, 2005: Jovian atmospheric dynamics: An update after *Galileo* and *Cassini*. *Rep. Prog. Phys.*, **68**, 1935–1996.
- Williams, G. P., 1978: Planetary circulations: 1. Barotropic representation of Jovian and terrestrial turbulence. *J. Atmos. Sci.*, **35**, 1399–1426.